DOI: 10.1002/cbic.200800600

Development and Biological Evaluation of a Novel Aurora A Kinase Inhibitor

Teresa Sardon,[a] Thomas Cottin,[b] Jing Xu,[b] Athanassios Giannis,*[b] and Isabelle Vernos*[a, c]

The aurora kinase family groups several serine/threonine kinases with key regulatory functions during cell division. The three mammalian members, aurora A, B and C, are frequently over-expressed in human tumors and the aurora A gene is located in a genomic region frequently amplified in breast and colon cancer. All these data have fuelled the idea that aurora kinases are promising targets for anticancer therapy. Indeed some inhibitory compounds are currently being evaluated in clinical trials. However, it was recently shown that mutations in the targeted kinase can confer resistance to a broad range of inhibitors and render patients resistant to treatments. Moreover, aurora A over-expression results in increased resistance to antimitotic agents. The development of new compounds targeting aurora A is therefore highly relevant. We describe here the synthesis of three novel aurora kinase inhibitors, TC-28, TC-34 and TC-107. We report their properties as aurora inhibitors in vitro and their effect on human tissue culture cell lines. Interestingly, our results show that TC-28 has properties compatible with the specific inhibition of aurora A, in vivo.

Introduction

Correct cell division is critical for the health and survival of cells and organisms. It involves a full intracellular reorganization and the formation of a microtubule-based apparatus, the bipolar spindle, which segregates the two copies of the chromosomes between daughter cells. Errors in this process result in the formation of cells with abnormal chromosome content—called aneuploidy—and lead to cell death or actively contribute to or even drive tumor development.[1] Aneuploidy is indeed a common characteristic of human solid tumors. To ensure the accuracy of chromosome segregation, cells have developed sophisticated regulatory networks that monitor and drive the orderly progression of events. These networks involve several members of the NIMA, polo-like and aurora kinase families.[2]

The aurora kinase family comprises three closely related serine/threonine kinases in metazoans named aurora A, B and C. All of them are regulators of various cell cycle related events from the G2 phase through to cytokinesis, including centrosome duplication, spindle assembly, chromosome bi-orientation and segregation and cytokinesis.[3]

The specific functions attributed to aurora A and B are tightly coupled to their distinctive localization at critical cell-cycle points. Aurora B (AurB) localizes to the kinetochores and to the spindle midzone in anaphase whereas aurora A (AurA) localizes to the centrosome and spindle poles. Recently AurA was shown to control cilia disassembly required for re-entry into the cell cycle.[4]

The aurora kinases have been linked to cancer in several ways.[5–7] In humans, the gene for AurA maps to a region 20q13 that is commonly amplified in primary tumors and cancer cell lines. In addition, AurA is over-expressed in several solid tumors. Interestingly, AurA amplification has been shown to induce resistance to taxol, a cytotoxic drug commonly used in cancer therapy.[8,9] AurA exogenous expression also promotes tumorigenic transformation of human and rodent cells in vitro and in vivo. Finally, certain AurA alleles have a higher incidence in tumor samples and cause enhanced tumorigenicity and genetic instability when expressed in cell lines.

The potential for targeted anticancer therapies has therefore promoted a strong interest in developing small-molecule inhibitors against the aurora kinases.[10–12] The most successful approaches based on the development of ATP-competitor derivatives have generated a few small-molecule inhibitors for the aurora kinases, including ZM447439, hesperadin, VX680, AZD1152 and MLN80545. In most cases, these compounds are not highly specific for any of the aurora kinases or even for other kinase families. ZM447439, hesperadin and VX680 inhibit both aurora A and B in vitro with various efficiencies, but they induce cellular phenotypes more compatible with the inhibition of AurB in vivo. MLN8054[13,14] is to date the only compound that shows both a >40-fold higher selectivity for AurA

[a] Dr. T. Sardon, Prof. Dr. I. Vernos
CRG-Cell and Developmental Biology Program
Parc de Recerca Biomedica de Barcelona
c/Dr. Aiguader 88, 08003 Barcelona (Spain)
Fax: (+34) 93-3160099
E-mail: isabelle.vernos@crg.es

[b] T. Cottin, J. Xu, Prof. Dr. A. Giannis
Institute for Organic Chemistry, University of Leipzig
Johannisallee 29, 04103 Leipzig (Germany)
Fax: (+49) 341-973-6599
E-mail: giannis@uni-leipzig.de

[c] Prof. Dr. I. Vernos
ICREA (Institució Catalana de Recerca i Estudis Avançats)
Barcelona (Spain)

Supporting information for this article is available on the WWW under http://dx.doi.org/10.1002/cbic.200800600.

 © 2009 Wiley-VCH Verlag GmbH & Co. KGaA, Weinheim

in vitro and cellular phenotypes that are compatible with AurA inhibition in vivo.

The promising tumor growth inhibitory activity of some of these compounds in nude mice has strengthened the idea that some of them could be useful for cancer therapy either used alone or in combination with other drugs.[15,16] Indeed, MLN8054 and VX-680 have recently entered clinical trials although the outcome is not yet available.[5]

Although there are precedents demonstrating the usefulness of cell cycle kinase inhibitors for the treatment of cancer,[17] clinical resistance can arise during treatment through adaptive mutations in the targeted kinase, which prevent inhibitor binding.[18] It was recently reported that a similar mechanism might confer resistance against inhibitory compounds targeting serine/threonine kinases.[19] One possible solution could be to develop multiple compounds targeting the same protein kinase.

We describe here the synthesis of three ATP-competitive inhibitors, TC-28, TC-34 and TC-107. We report their properties as aurora inhibitors in vitro and their effect on human tissue culture cells and show that TC-28 has properties compatible with AurA inhibition in vivo.

Results and Discussion

Development of new aurora kinase inhibitors

Quinazoline is a favored lead structure for ATP-analogue inhibitors and many inhibitors based on this scaffold have been characterized.[20] We therefore chose this scaffold for the synthesis of derivatives. The ATP-binding pocket of the aurora kinases consists of a N-terminal β-sheet domain and a C-terminal α helix. The substrates and ATP are bound in the presence of Mg^{2+}. The kinase domains of the three aurora kinases share high sequence similarities. They also show various degrees of similarities with the kinase domains of more divergent kinase families. However, some small differences can be used for the creation of selective inhibitors. The ATP-binding pocket of aurora A is very hydrophobic. An important possibility to induce selectivity is the so-called fluorophenyl pocket. This region is formed by the amino acids Ala160, VaL147, Leu210 and Glu211,[21] and it has a hydrophobic character. It gets its name from a fluorophenyl moiety that inhibits MAP kinases by targeting this pocket. In many other kinases this domain is not accessible because of the presence of amino acids with larger side chains in this region or amino acids with side chains that make this pocket less hydrophobic. For this reason, in the 2-position of some of the quinazolines a furyl-substituent was introduced to obtain selectivity. Compared with other kinases the ATP-binding pocket of AurA shows the insertion of an additional amino acid, Gly216. This insertion leads to a change of the conformation of the adenosine-binding region and decreases its size. This change avoids the formation of hydrogen bonds between the ATP ribose hydroxyl groups and Thr217, which is present in other kinases. For this reason small substituents were introduced in the 4- and 6-positions. In the small ATP-binding pocket of AurA they should bind better than sterically high-demanding derivatives.[19]

A library of quinazolines with 15 compounds was synthesized and their activity against AurA and AurB was determined at the European Molecular Biology Laboratory facility (EMBL, Heidelberg, Germany). Three compounds (TC-28, TC-34 and TC-107) produced selective inhibition of AurA versus AurB

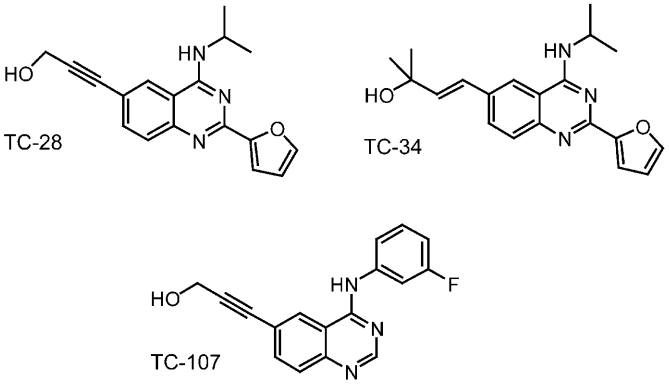

(Table 1) and were further investigated against receptor tyrosine kinases with an assay based on the ELISA principle (Table 1). Encouragingly, TC-28 did not inhibit any of the tested tyrosine kinases ($IC_{50} > 100$ μM).

Table 1. IC_{50} values of TC-28, TC-34 and TC-107 against AurA, AurB and a panel of other selected kinases.

IC_{50} [μM]	TC-28	TC-34	TC-107
aurora A	2.7	1.9	0.052
aurora B	[a]	16.2	4.5
EGFR	[a]	[a]	[a]
IGFR	[a]	41.5	[a]
KDR	[a]	8.2	2.9
Flt-4	[a]	4.2	1.5
FGFR	[a]	[a]	[a]
Tie-2	[a]	[a]	[a]

[a] > 100 μM.

TC-28 delays G2M progression in human tumor cells

Previous studies have shown that the treatment of cells with small-molecule inhibitors for aurora kinase results in the accumulation of cells with a DNA content of $> 4n$.[22–25] We first examined the cell-cycle profiles of HeLa cells incubated for 24 h in medium containing increasing concentrations of any of the three compounds, TC-28, TC-34 or TC-107 by flow cytometry. We used the previously characterized aurora inhibitor, ZM447439 (ZM1; 2 μM) as positive control.[23] Consistent with published results, treatment with ZM1 increased the proportion of cells with 4*n* and 8*n* DNA content (Figure 1 and Table 2). HeLa cells incubated with TC-28 showed a dose-dependent increase in the proportion of cells with more than 2*n* DNA content, but more than 4*n* DNA content was not ob-

 © 2009 Wiley-VCH Verlag GmbH & Co. KGaA, Weinheim

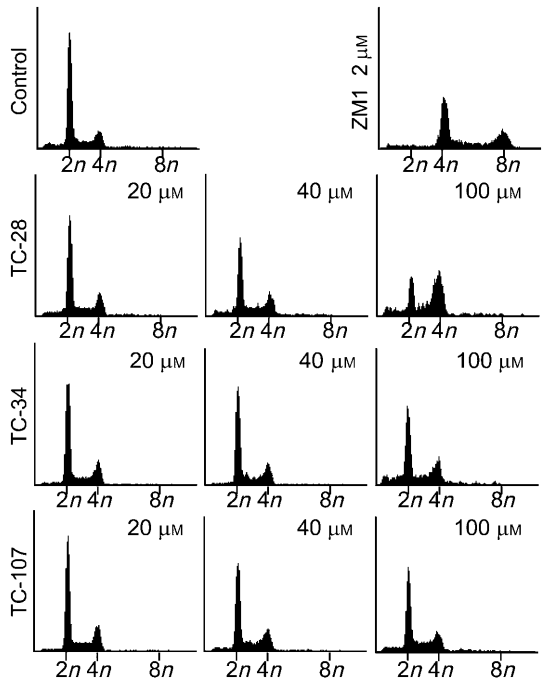

Figure 1. DNA profiles of HeLa cells treated with DMSO (control), ZM1 (2 μM) or increasing concentrations of TC-28, TC-34 or TC-107 for 24 h were evaluated by flow cytometry; 2*n*, 4*n* and 8*n* reflect relative DNA content and represent diploid, tetraploid and multinucleated cells, respectively.

Table 2. Percentage of cells in G1, S, G2M and with more than 4*n* DNA content as calculated from Figure 1.

% of cells	$<2n$	2*n*	$2<n<4$	4*n*	$>4n$
control	6.8	64.0	15.7	13.6	0.8
ZM1 (2 μM)	3.0	1.2	2.8	51.1	43.5
TC-28					
20 μM	7.6	55.2	17.5	19.0	1.3
40 μM	10.5	47.2	20.0	21.2	1.8
100 μM	10.0	21.4	25.2	41.8	1.5
TC-34					
20 μM	4.4	58.5	17.6	19.2	0.7
40 μM	3.8	58.5	17.7	19.9	3.8
100 μM	13.8	48.4	15.5	20.8	2.1
TC-107					
20 μM	2.5	56.7	17.7	19.9	3.8
40 μM	4.5	55.2	20.4	19.8	0.8
100 μM	7.6	50.2	23.3	18.7	1.0

served (Figure 1 and Table 2). Neither TC-34 nor TC-107 altered the distribution of cells in the different cell-cycle stages. Incubation for longer periods of time (48 h) with any of the three compounds resulted in extensive cell death.

The high proportion of 8*n* DNA containing cells observed after ZM1 treatment has been related to AurB inhibition, which is also characterized by a decrease in the levels of histone H3 (HH3) phosphorylation on Ser10.[23] Phosphorylation at this site is frequently used as a marker for AurB activity. The lack of 8*n* cell accumulation following treatment with any of the TC compounds suggests that none of them inhibited AurB activity in vivo. To confirm this hypothesis we studied HH3 phosphorylation levels in mitotic cells treated with the different compounds for 20 h.

As shown in Figure 2, ZM1 treatment strongly reduced HH3 Ser10 phosphorylation, which is consistent with published data.[23] By contrast, treatment with any of the TC compounds

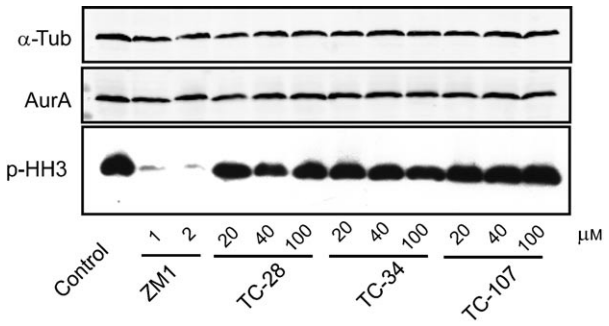

Figure 2. Effect of the different compounds on histone H3 phosphorylation at Ser10. HeLa cells were treated with ZM1 or the different TC compounds and synchronized in mitosis with nocodazole. Histone H3 phosphorylation degree (p-HH3) was determined by Western blot analysis. AurA and α-tubulin (α-Tub) levels were used as synchronization and loading controls.

had no effect at any of the concentrations tested; this supports the idea that AurB activity is unaffected in vivo. These results diverge from the efficient AurB inhibition observed in vitro for TC-34 and TC-107, and could indicate that problems in permeability or solubility prevent the inhibitory activity of these compounds at the cellular level.

The increase in the proportion of cells with more than 2*n* DNA content could be due to several causes. It could be brought about by multiple cycles of DNA replication or by cytokinesis errors, as shown for cells treated with other aurora inhibitors.[22,24] To determine the primary cause for the phenotype produced by TC-28 and examine whether TC-34 or TC-107 interfere with mitosis, we examined live cells by time-lapse video microscopy. To visualize DNA and microtubules we used a stable HeLa cell line coexpressing H2B–GFP and mRFP–α-tubulin fusion proteins. Cells were placed in medium containing 2 μM ZM1 or 40 μM of any of our three compounds, and imaged every 3 or 4.5 min for 16–24 h (Figure 3). The resulting time-lapse images were used to determine the following parameters: 1) the percentage of cell death among nondividing cells (Figure 4A), 2) the percentage of cells entering mitosis (Figure 4B), 3) the outcome of mitosis: normal division (cell division), return to interphase without chromatin segregation and without dividing (no division), cytokinesis failure (division errors), cell death without resolving mitosis (cell death; Figure 4C), and 4) the length of time spent in mitosis (TIM), which is defined as the interval between DNA condensation and anaphase resolution (Figure 4D).

Control cells, which were plated in medium containing DMSO, were healthy throughout the observation time. An average of 5.4% of the cells entered mitosis per hour (Figure 4B) and almost all of them (90.3%) were able to divide successfully with an average TIM of 39 min (median; Figure 4D). Treatment with ZM1 decreased the number of cells

 © 2009 Wiley-VCH Verlag GmbH & Co. KGaA, Weinheim

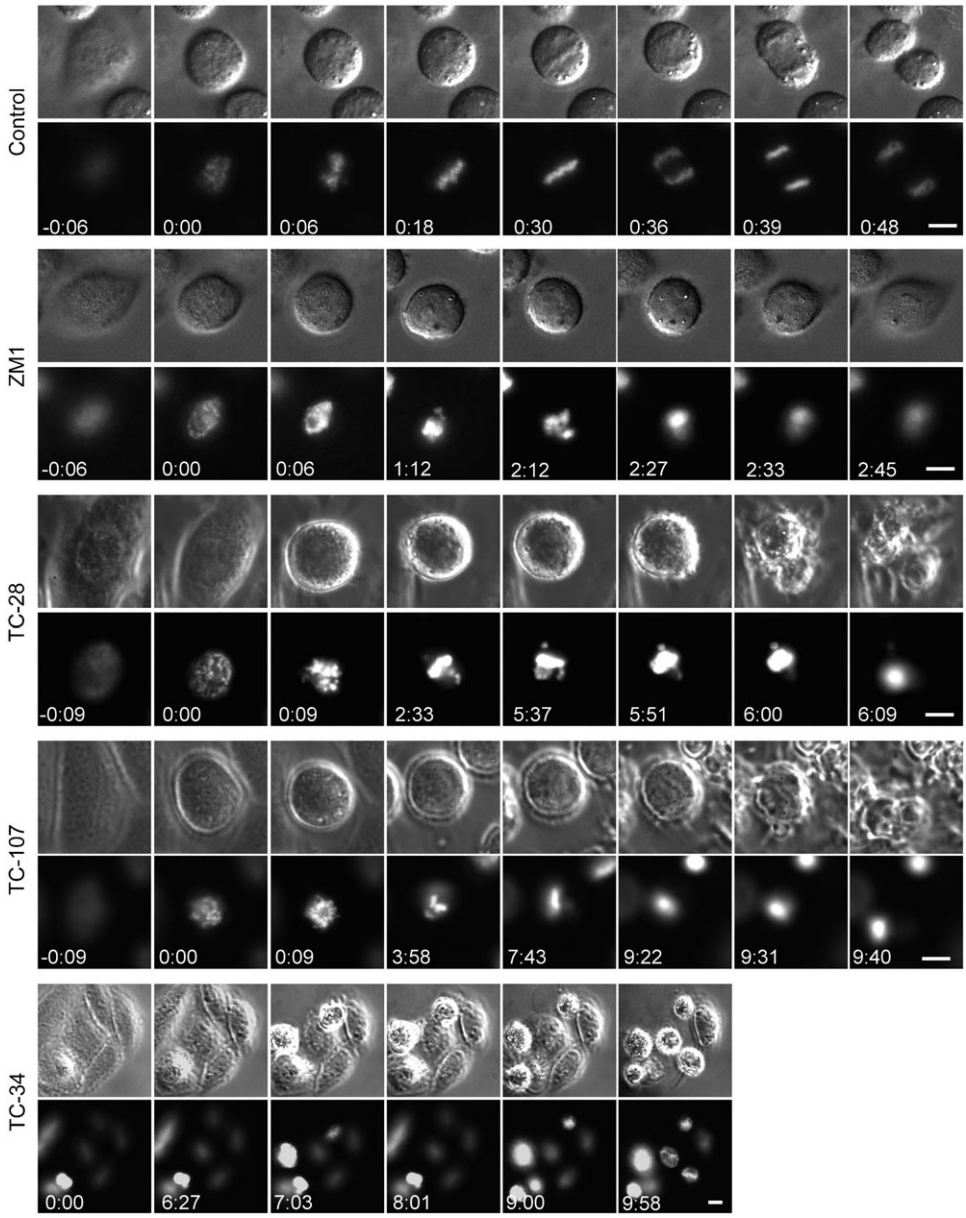

Figure 3. Images from time-lapse analysis of cells treated with DMSO, ZM1, TC-28, TC-34 or TC-107. HeLa cells expressing GFP–histone 2B and mRFP–α-tubulin (lower row in each set) were incubated in medium containing DMSO (control), ZM1 (2 μM), TC-28 (40 μM), TC-107 or TC-34. Images were captured for a period of 16–24 h by using a time-lapse imaging system. In each panel the upper row shows the phase-contrast images and the lower row the GFP signal; scale bar: 10 μm. Also, see movies in the Supporting Information.

entering mitosis by half. In agreement with published data, ZM1 also increased the TIM to 306 min.[23] During the time in mitosis, cells had problems in reaching metaphase, and 76% decondensed their DNA and went back to interphase without chromosome segregation. Incubation of cells with TC-28 also reduced the number of cells entering mitosis and increased the TIM (median 375 min), but unlike cells treated with ZM1, all the TC-28 treated cells died either without returning to interphase or right after an asymmetric segregation.

In addition to these mitotic phenotypes, we observed that TC-34 induced extensive cell death (Figure 4 A), so that after 11 h incubation almost no cells remained in the dish. During this period of observation the few cells that entered mitosis completed it successfully.

TC-107 also resulted in an increase in cell death although not as strongly as TC-34 (Figure 4 A). In the remaining population an average of 1.4% of cells entered mitosis per hour, half of these completed cell division, but with a broadly variable TIM. The other half died without going back to interphase.

It has been reported that inhibition of AurB kinase activity by over-expressing a "dead" kinase mutant produces an increase in the proportion of cells with 4*n* and 8*n* DNA content due to a failure in cell division. By contrast, over-expression of a dead kinase AurA does not affect the DNA-content profile. The fact that ZM1 mimics the AurB phenotype suggests in vivo AurB inhibition by this compound.[23] Our data suggest that TC-28 does not inhibit AurB in vivo and show that it induces defects compatible with AurA inhibition.[17,23] TC-34 and TC-107 had a strong effect on cell viability, which were independent of mitosis and not related to defects that could suggest inhibition of aurora kinases. Since TC-34 and TC-107 also have inhibitory effects on other kinases in vitro whereas TC-28 has none, we decided to continue our studies with TC-28.

TC-28 interferes with bipolar spindle formation

To get a better idea about the defects causing cell division failure in cells treated with TC-28, we examined fixed cells to better visualize the chromosomes and the microtubules. The stable HeLa cells expressing GFP–histone and mRFP–α-tubulin were incubated with TC-28 (40 μM), ZM1 (2 μM) or DMSO (control) for 24 h, fixed in cold methanol and mounted. In parallel, standard HeLa cells were treated in the same way. Cells were fixed and processed for immunofluorescence with anti-tubulin antibodies to visualize the microtubules and Hoechst 33342 to stain the DNA. Mitotic cells were examined and classified into the different mitotic phases and other abnormal states (Figure 5 A).

 © 2009 Wiley-VCH Verlag GmbH & Co. KGaA, Weinheim

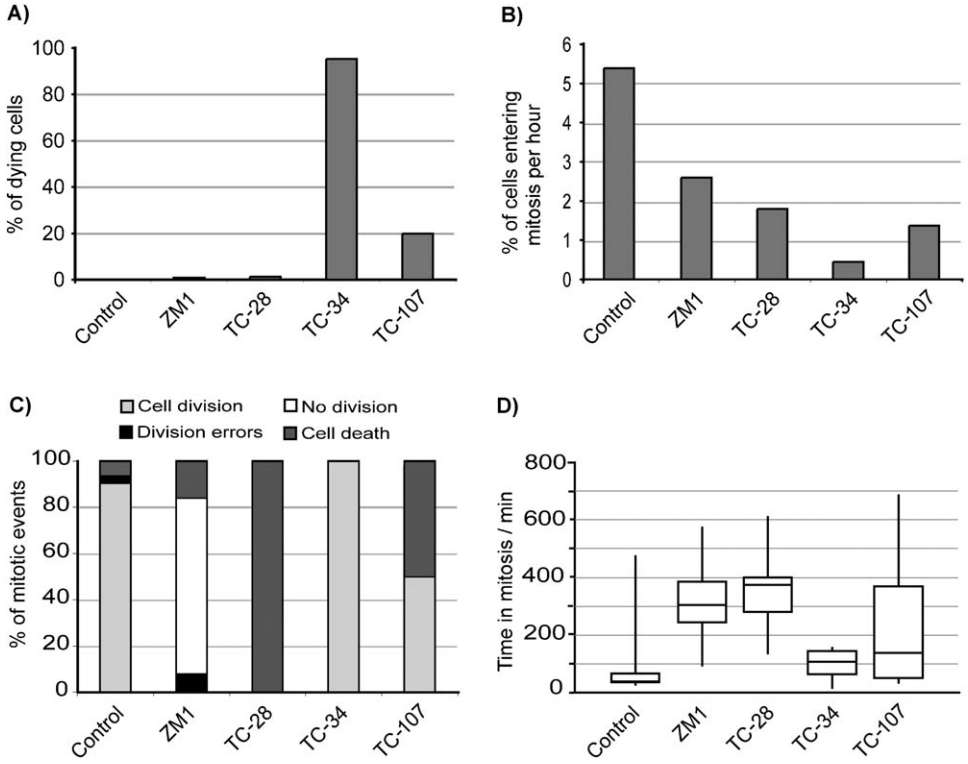

Figure 4. Quantification of the phenotypes observed during the time-lapse recording of cells treated with the different compounds. A) Bar graph showing the mean percentage of nondividing cells that died over the period of the time-lapse recording. The values obtained from more than six fields from two independent experiments were averaged. B) Average percentage of cells entering mitosis per hour of observation. The percentage of cells entering mitosis in each filmed field was divided by the number of filming hours. The values obtained from more than six fields from two independent experiments were averaged. C) Outcome of cells entering mitosis. Cells entering mitosis were followed carefully over time and each mitotic event was classified in one of the following four categories: normal division (cell division), return to interphase without chromosomes segregation and without dividing (no division), cytokinesis failure (division errors), and cell death without resolving mitosis (cell death). D) Box plots show the time spent in mitosis in the presence of 2 μM ZM1 or 40 μM TC-28, TC-34 or TC-107. Values obtained from more than six fields from two independent experiments were averaged.

Cells incubated with ZM1 showed a strong increase in the number of mitotic cells with chromosome alignment defects in metaphase: although most chromosomes aligned on the metaphase plate, several were in the proximity of the spindle poles (Figure 5). A high percentage of cells were multinucleated. These data are consistent with the reported phenotypes for AurB inhibition or silencing.

By contrast, cells treated with TC-28 showed a large proportion of abnormal mitotic spindles (defined as those that did not display canonical bipolar spindle formation: monopolar, multipolar and other aberrant structures).

Cells incubated with TC-34 or TC-107 and in mitosis did not show significant defects in spindle assembly or chromosome alignment (data not shown).

We conclude that TC-28 has a strong effect on mitotic progression and induces phenotypes that are compatible with AurA inhibition.

TC-28 impairs cilia disassembly

Recent studies have shown that AurA has some nonmitotic roles. It localizes at the basal body of cilia and its activation promotes cilia disassembly, which is a prerequisite for cells to re-enter the cell cycle and go through a new round of division. Depletion of AurA by siRNA treatment or the use of a small molecule inhibitor targeting AurA were shown to substantially limit serum-induced disassembly of cilia.[4] Since this is an AurA specific function we decided to use this experimental approach to test the specificity of TC-28 for AurA inhibition.

The hTERT-RPE1 cells were plated at 50% confluence in medium without serum. After 48 h more than 80% of the cells had clearly visible cilia as detected by immunofluorescence with an anti-acetylated α-tubulin antibody. As previously described, changing the culture medium to one containing fetal bovine serum (10%) caused cilia disassembly in the first two hours after serum stimulation (Figure 6). Pretreatment of cells with ZM1 (1–2 μM) did not have any effect on cilia disassembly; by contrast, it was strongly inhibited in cells pretreated with TC-28 (40 μM; Figure 6).

Conclusions

To design novel ATP competitors that show specificity for the inhibition of AurA we examined carefully the structure of the kinase domains of the three aurora kinases, and searched for any small difference that could be useful for the creation of selective inhibitors.

Based on this study and by using a quinazoline scaffold as a lead structure a furyl-substituent was introduced in the 2-position and small substituents were introduced in the 4- and 6-positions. Among the synthesized compounds three showed selective inhibition of AurA compared to AurB in vitro.

Although TC-34 and TC-107 compromise cell viability we did not observe specific effects on mitotic cells either morphologically or on HH3 Ser10 phosphorylation. This suggests that these two compounds have solubility problems or might not enter into cells efficiently.

TC-28 promoted mitotic arrest compatible with AurA inhibition in vivo. To determine more accurately whether this compound inhibits AurA specifically, we examined whether it inhibited the disassembly of the primary cilia, which is a process that has been shown to be specifically regulated by AurA. Our results show that TC-28 indeed inhibits this process; this indi-

 © 2009 Wiley-VCH Verlag GmbH & Co. KGaA, Weinheim

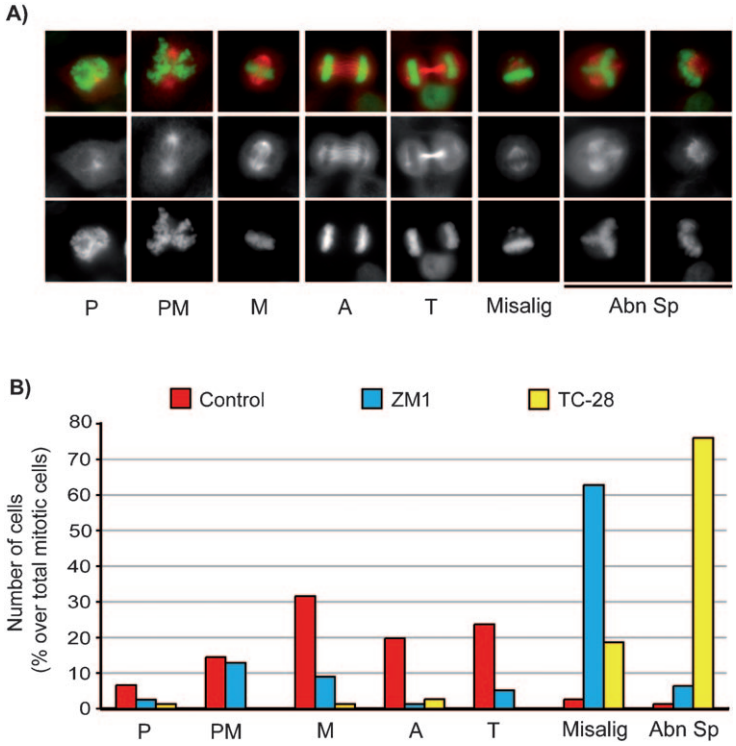

Figure 5. Mitotic phenotypes of cells incubated in the presence of the different compounds. A) HeLa cells constitutively expressing GFP–histone H2B and mRFP-conjugated α-tubulin were incubated for 24 h in the presence of DMSO or ZM1 (2 μM) or TC-28 (40 μM), fixed and examined. Mitotic cells were scored and classified according to the different categories shown. Representative images for the different categories are shown: prophase (P), prometaphase (PM), metaphase (M), anaphase (A), telophase (T), metaphase spindles with lagging chromosomes (Misalign) and abnormal spindles (Abn Sp), which were defined as mitotic structures whose microtubules (MT) are not organized in a canonical bipolar spindle; MTs are in red and DNA is in green. B) Quantification of the number of cells in the different categories defined in A). Untreated cells (red), cells treated with ZM1 (blue) and TC-28 (yellow).

cates that the compound inhibits AurA in vivo. Consistently, docking analysis indicates that the inhibitor could easily bind in the same region as the ATP (Figure S1 in the Supporting Information). The next goal will be to enhance the potency and solubility of TC-28 to generate a specific AurA inhibitor that could have useful clinical applications.

Experimental Section

Chemistry

Scheme: Synthesis of the 2-(2-furyl)-substituted derivatives commenced with anthranilic acid amide **1**. Introduction of iodine in 5-position was followed by the coupling of furan-2-carbonyl chloride to the anilino-nitrogen and ring closure to quinazolinone **5** under basic conditions.[26] Derivatives with no substituent in the 2-position were prepared by the condensation of 2-amino-5-iodobenzoic acid (**3**) and formamidine hydrochloride.[27] The obtained quinazolinones **4** and **5** were further converted to the 4-chloroquinazolines **6** and **7** under reflux in phosphoryl trichloride or in thionyl chloride with catalytic amounts of DMF, respectively.[28,29] Nucleophilic aromatic substitution furnished the 4-aminoquinazolines **8**–**10** in good yields[29,30] (Scheme 1). Furthermore, derivatives were prepared so that diversity in the 4-position was obtained (Table 3). The Suzuki coupling of quinazolinone **5** with 4-methoxyphenylboronic acid, followed by reflux in phosphoryl trichloride gave 4-chloroquinazoline **12**.[28,31] Thus, L-serine methylester and 2-aminoethanol were introduced as side-chains by aromatic substitution reactions.[32] The propargyl alcohol derivative **15** was obtained by a Sonogashira reaction.

Different well-known palladium-catalyzed coupling reactions provided a variety of 6-substituted quinazolines. By

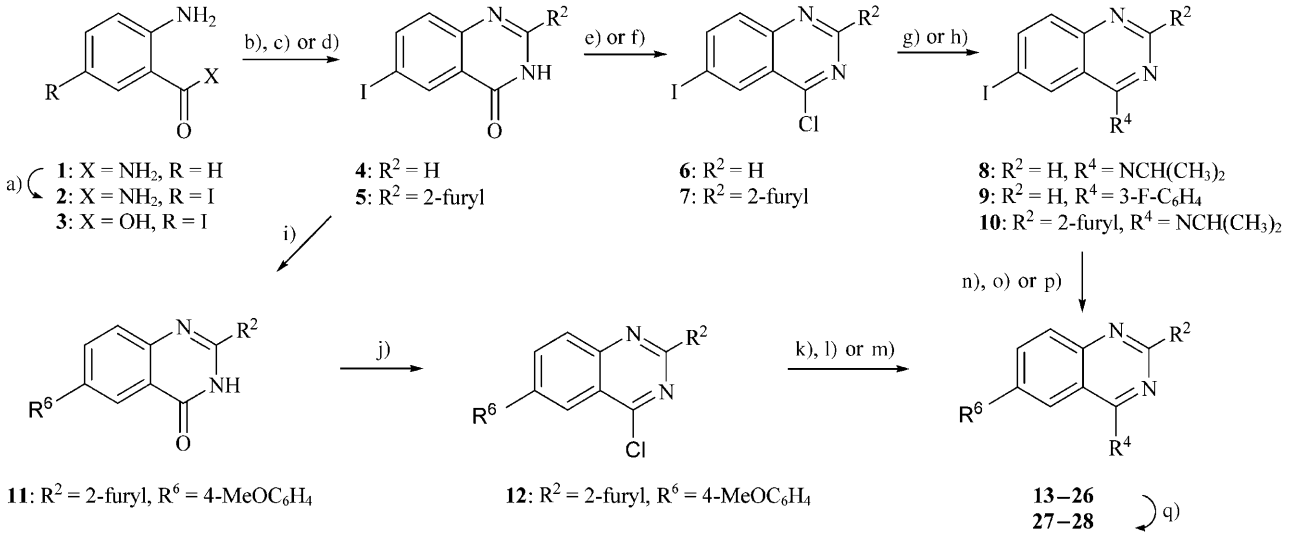

Scheme 1. Synthesis of the quinazoline derivatives. a) I_2, $NaHCO_3$, H_2O, room temperature, 18 h, 82%; b) furan-2-carbonyl chloride, Et_3N, THF, room temperature, 2 h, 99% (X = N); c) 5% NaOH, EtOH, reflux, 5 min, 78% (X = N); d) formamidine hydrochloride, 210 °C, 20 min, 86% (X = O); e) $POCl_3$, reflux, 3 h, 86%, R^1 = 2-furyl; f) $SOCl_2$, DMF, reflux, 4 h, 66%; R^1 = H; g) *i*$PrNH_2$, 35 °C, 18 h, 98%; h) 3-fluoroaniline, HCl, *i*PrOH, reflux, 30 min, 90%; i) 4-methoxyphenylboronic acid, K_2CO_3, $Pd(OAc)_2$, dioxane/water (3:1), reflux, 2 h, 62%; j) $POCl_3$, reflux, 3 h, 45%; k) 2-aminoethanol, *i*PrOH, reflux, 30 min, 100%; l) L-serinmethylester hydrochloride, Et_3N, THF, room temperature, 24 h, 56%; m) prop-2-yn-1-ol, Et_3N, $Pd(PPh_3)_2Cl_2$, CuI, DMF, 50 °C, 18 h, 39%; n) boronic acid, K_2CO_3 or Cs_2CO_3, $Pd(PPh_3)_4$ or $Pd(OAc)_2$, dioxane/water (3:1), reflux, 30 min to 2 h, 76–96%; o) alkene, Et_3N, $Pd(OAc)_2$, (*o*-Tol)$_3$P, acetonitrile, 100 °C, 48–72 h, 63–87%; p) prop-2-yn-1-ol, Et_3N, $Pd(PPh_3)_2Cl_2$, dppf, DMF, 50 °C, 16–18 h, 61–93%, q) acid chloride, Et_3N or DIPEA, THF, room temperature or 50 °C, 3–18 h, 74–81%.

 © 2009 Wiley-VCH Verlag GmbH & Co. KGaA, Weinheim

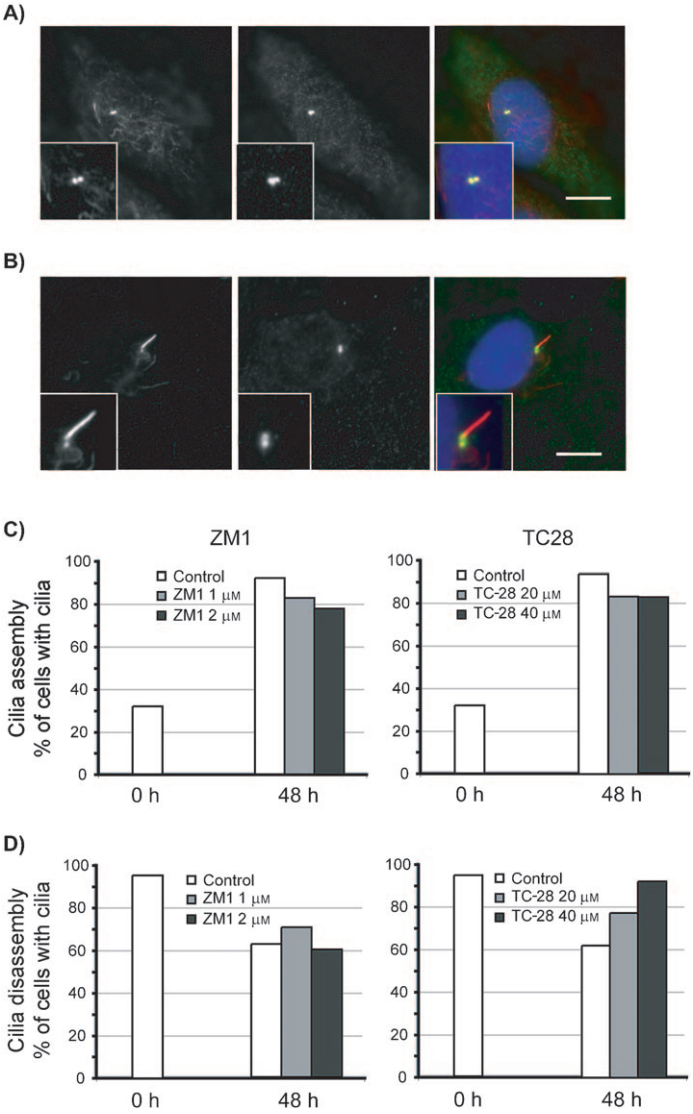

Figure 6. TC-28 blocks cilia disassembly. A) Representative immunofluorescence images of interphase RPE cells. The anti-acetylated tubulin and anti-α-tubulin antibody decorate the centrosome of actively growing RPE cells. B) Serum starved RPE cells develop cilia from one of the two centrioles. The anti-acetylated tubulin antibody decorates both centrioles, including the basal body and its connected cilium. Acetylated tubulin is in red, α-tubulin in green and the DNA is in blue in the merge images. C) Quantification of the number of cells forming a cilium when serum starved in the presence of the compounds. No differences were observed among cells incubated with the different compounds. Graphs show a representative experiment repeated three times. D) Quantification of the number of cells that lost cilia when they were transferred to a medium containing serum and the compounds indicated after serum starvation. Cilia disassembly was impaired in the presence of TC-28. Graphs show a representative experiment repeated three times.

Suzuki coupling with $Pd(PPh_3)_4$ and $Pd(OAc)_2$ as catalysts with the solvent system dioxane/water, 6-aryl substituted derivatives were obtained in high yields.[31] In addition, N-acylation of derivative **18** led to further structural diversity. The Heck reaction furnished three derivatives with good yields including TC-34, for which $Pd(OAc)_2$ was used as catalyst and $(o\text{-Tol})_3P$ as ligand.[33] Finally, a Sonogashira reaction with propargyl alcohol and $Pd(OAc)_2$/dppf as catalyst yielded TC-107 and TC-28.

Table 3. Derivatives generated by modifications in the 4-position.

	R^2	R^4	R^6
13	2-furyl	NH–$(CH_2)_2OH$	4-MeO–C_6H_4
14	2-furyl	L-serinmethylester	4-MeO-C_6H_4
15	2-furyl	C≡CCH_2OH	4-MeO–C_6H_4
16	2-furyl	$NCH(CH_3)_2$	4-MeO–C_6H_4
17	2-furyl	$NCH(CH_3)_2$	3-CHO–C_6H_4
18 (TC-34)	2-furyl	$NCH(CH_3)_2$	(*E*)-CH=$CHC(CH_3)_2OH$
19	2-furyl	$NCH(CH_3)_2$	(*E*)-CH=$CHCOOC(CH_3)_3$
20 (TC-28)	2-furyl	$NCH(CH_3)_2$	C≡CCH_2OH
21	H	$NCH(CH_3)_2$	4-MeO–C_6H_4
22	H	3-F–C_6H_4	4-MeO–C_6H_4
23	H	3-F–C_6H_4	3-NH_2–C_6H_4
24	H	3-F–C_6H_4	(*E*)-CH=$CHC(CH_3)_2OH$
25 (TC-107)	H	3-F–C_6H_4	C≡CCH_2OH
26	2-furyl	$NCH(CH_3)_2$	3-NH_2–C_6H_4
27	2-furyl	$NCH(CH_3)_2$	3-$NHCOCH_3$–C_6H_4
28	2-furyl	$NCH(CH_3)_2$	3-$NHCOCCl_3$–C_6H_4

[a] Catalyst system yielded TC-107 and TC-28.[34]

Experimental part: All reagents were commercially obtained from Acros, Aldrich, Alfa Aesar and Fluka and used without further purification. Melting points were measured with a Boetius-micro hot stage and are uncorrected. The ^1H and ^{13}C NMR spectra were recorded by using a Varian Gemini 200 (200 MHz for ^1H NMR; 50 MHz for ^{13}C), a Varian Gemini 300 (300 MHz for ^1H NMR; 75 MHz for ^{13}C NMR) and Bruker Advance-DRX 400 (400 MHz for ^1H NMR; 100 MHz for ^{13}C NMR); the residual solvent peak was used as an internal reference. HRMS were obtained on a Bruker Daltonics APEX II (for ESI) and on a Meß- und Analysentechnik Bremen MAT8035 (EI). Reactions involving moisture-sensitive reactants were performed in flame-dried glassware under an argon atmosphere; reactants were added by using a syringe. Flash column chromatography was performed on silica gel (Acros 60A, 0.035–0.070 mm) and analytical TLC on precoated silica gel plates (Merck 60 F254, 0.25 mm).

*2-Amino-5-iodobenzamide (**2**)*: Powdered iodine (11.7 g, 46.2 mmol) was added portion-wise over 1 h to a stirred solution of 2-aminobenzamide (**1**; 5.72 g, 42.0 mmol) and $NaHCO_3$ (3.52 g, 42.0 mmol) in water (1.3 L). The solution was stirred, overnight, at room temperature. Afterwards $NaHSO_3$ (0.87 g, 8.40 mmol) was added. The solution was extracted with ethyl acetate (3×800 mL). After being dried with Na_2SO_4 the organic phase was removed under reduced pressure. The crude product was recrystallized with water/methanol mixture (10:1, *v/v*, 100 mL) to yield **2** (9.07 g, 34.6 mmol, 82%) as white crystals; m.p. 197–198 °C; ^1H NMR (300 MHz, [D_6]DMSO): $\delta = 6.57$ (d, $J = 8.7$ Hz, 1 H, arom), 6.74 (s, 2 H, NH_2), 7.19 (s, 2 H, $CONH_2$), 7.42 (dd, $J = 8.7$, 1.8 Hz, 1 H, arom), 7.84 (d, $J = 2.1$ Hz, 1 H, arom); ^{13}C NMR (75 MHz, [D_6]DMSO): $\delta = 74.5$, 116.1, 119.0, 136.5, 139.9, 149.8, 169.9; HR EI-MS: calcd for ($C_7H_7IN_2O$): 261.96032, found: 261.95953.

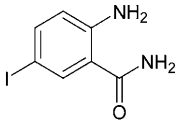

N-*(2-Carbamoyl-4-iodophenyl)furan-2-carboxamide (**2a**)*: Triethylamine (2.19 mL, 15.7 mmol) and furan-2-carbonyl chloride (0.77 mL, 7.86 mmol) were added by using a syringe to a solution of 2-amino-5-iodobenzamide (**2**; 2.06 g, 7.86 mmol) in THF (23 mL). After 2 h (TLC control) the solvent was removed under reduced pressure. The residual solid was washed with cold ethanol to yield pure **2a** (2.76 g, 7.75 mmol, 99%) as a white solid; m.p. 218–

 © 2009 Wiley-VCH Verlag GmbH & Co. KGaA, Weinheim

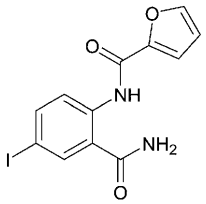

220 °C; ^{1}H NMR (300 MHz, [D$_6$]DMSO): δ = 6.75 (dd, J = 3.0, 3.0 Hz, 1 H, arom), 7.26 (d, J = 3.0 Hz, 1 H, arom), 7.90 (dd, J = 8.7, 1.8 Hz, 1 H, arom), 7.99 (s, 1 H, arom), 8.22 (d, J = 1.8 Hz, 1 H, arom), 8.46 (d, J = 9.0 Hz, 1 H, arom), 8.49 (s, 2 H, NH$_2$), 12.72 (s, 1 H, NH-CO); ^{13}C NMR (75 MHz, [D$_6$]DMSO): δ = 87.2, 113.4, 116.1, 122.2, 122.8, 137.5, 139.8, 141.6, 146.9, 148.2, 156.4, 170.2; HR ESI-MS: calcd for $C_{12}H_9IN_2O_3Na$: 378.95555 [M+Na]$^+$, found: 378.95501.

*2-(Furan-2-yl)-6-iodoquinazolin-4(3*H*)-one (**5**)*: A solution of *N*-(2-carbamoyl-4-iodophenyl)furan-2-carboxamide (**2a**; 2.76 g, 7.75 mmol) in NaOH (5 %, 39 mL) and ethanol (20 mL) was refluxed for 5 min. After the solution was cooled to 0 °C a voluminous white precipitate was formed and filtered off. It was dried to yield pure **5** (2.05 g, 6.06 mmol, 78 %) as a white solid; m.p. 222–223 °C; ^{1}H NMR (300 MHz, [D$_6$]DMSO): δ = 6.75 (dd, J = 3.6, 3.3 Hz, 1 H, arom), 7.26 (d, J = 2.7 Hz, 1 H, arom), 7.91 (dd, J = 8.7, 2.1 Hz, 1 H, arom), 8.00 (s, 1 H, arom), 8.21 (d, J = 2.4 Hz, 1 H, arom), 8.45 (d, J = 9.3 Hz, 1 H, arom), 8.49 (s, 1 H, NH); ^{13}C NMR (75 MHz, [D$_6$]DMSO): δ = 87.2, 113.4, 116.1, 122.2, 122.8, 137.5, 139.8, 141.6, 146.9, 148.2, 156.4, 170.2; HR ESI-MS: calcd for $C_{12}H_8IN_2O_2$: 338.96305 [M+H]$^+$, found: 338.96250.

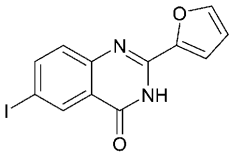

*4-Chloro-2-(furan-2-yl)-6-iodoquinazoline (**7**)*: A solution of 2-(furan-2-yl)-6-iodoquinazolin-4(3*H*)-one (**5**; 1.95 g, 5.76 mmol) in phosphoryl trichloride (50 mL) was refluxed for 3 h (TLC control). The white suspension became a clear solution. The excess of phosphoryl trichloride was removed under reduced pressure. The remaining solid was suspended in ethyl acetate (150 mL) and washed with NaOH solution (1 M; 5×100 mL). The combined aqueous phases were re-extracted with ethyl acetate (100 mL). The combined organic phases were washed with brine (150 mL) and dried over Na$_2$SO$_4$. After removal of the solvent under reduced pressure the crude product was purified by column chromatography (*n*-hexane/ethyl acetate, 5:1, *v*/*v*; R_f: 0.31) to yield **7** (1.77 g, 4.97 mmol, 86 %) as a yellow solid, m.p. 183–184 °C; ^{1}H NMR (300 MHz, [D$_6$]DMSO): δ = 6.79 (d, J = 3.6 Hz, 1 H, arom), 7.50 (d, J = 8.7 Hz, 1 H, arom), δ = 7.69 (d, J = 3.6 Hz, 1 H, arom), 8.05 (s, 1 H, arom), 8.11 (dd, J = 8.9, 2.3 Hz, 1 H, arom), 8.39 (d, J = 2.1 Hz, 1 H, arom); ^{13}C NMR (50 MHz, [D$_6$]DMSO): δ = 91.5, 112.7, 115.5, 122.8, 128.9, 134.2, 143.0, 144.5, 145.5, 147.1, 160.1, 150.0; HR ESI-MS: calcd for $C_{12}H_7ClIN_2O$: 356.92916 [M+H]$^+$, found: 356.92861.

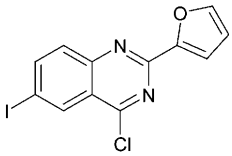

*2-(Furan-2-yl)-6-iodo-*N*-isopropylquinazolin-4-amine (**10**)*: A solution of 4-chloro-2-(furan-2-yl)-6-iodoquinazoline (**7**; 1.70 g, 4.70 mmol) and isopropylamine (1.02 mL, 11.9 mmol) in propan-2-ol (70 mL) was stirred, overnight, at 35 °C. The yellow suspension turned to a clear solution. After removal of the solvent under reduced pressure the crude product was purified by column chromatography (*n*-hexane/ethyl acetate, 3:1, *v*/*v*; R_f: 0.35) to yield **10** (1.77 g, 4.67 mmol, 98 %) as an orange-colored solid, m.p. 205 °C; ^{1}H NMR: (200 MHz, [D$_6$]DMSO): δ = 1.31 (d, J = 6.6 Hz, 6 H, CH(CH$_3$)$_2$), 4.61 (se, J = 6.8 Hz, 1 H, CH(CH$_3$)$_2$), 6.67 (dd, J = 3.4, 3.3 Hz, 1 H, arom), 7.25 (d, J = 2.5 Hz, 1 H, arom), 7.48 (d, J = 8.8 Hz, 1 H, arom), 7.89 (d, J = 2.6 Hz, 1 H, arom), 8.01 (dd, J = 8.8, 1.9 Hz, 1 H, arom), 8.09 (d, J = 7.6 Hz, 1 H, NH), 8.75 (d, J = 1.8 Hz, 1 H, arom); ^{13}C NMR (50 MHz, [D$_6$]DMSO): δ = 21.9 (2 C), 42.2, 89.9, 112.1, 112.9, 115.6, 129.5, 131.4, 141.0, 145.0, 148.9, 153.0, 153.6, 157.5; HR ESI-MS: calcd for $C_{15}H_{15}IN_3O$: 380.02598 [M+H]$^+$, found: 380.02529.

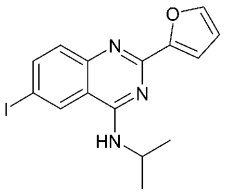

*2-(Furan-2-yl)-*N*-isopropyl-6-(4-methoxyphenyl)quinazolin-4-amine (**16**)*: A solution of 2-(furan-2-yl)-6-iodo-*N*-isopropylquinazolin-4-amine (**10**; 140 mg, 0.37 mmol), 4-methoxyphenylboronic acid (59 mg, 0.39 mmol) and potassium carbonate (306 mg, 2.21 mmol) in dioxane/water (3:1, *v*/*v*; 4.3 mL) was degassed with ultrasound for 10 min. After addition of tetrakis-(triphenylphosphin)-palladium(0) (8.5 mg, 7.38 μmol) the solution was refluxed for 30 min (TLC control). After the solution was cooled to room temperature, water (10 mL) was added and the solution was extracted with ethyl acetate (3×15 mL). The combined organic phases were washed with brine (15 mL) and dried over Na$_2$SO$_4$. After the solvent was removed under reduced pressure the crude product was purified by column chromatography (*n*-hexane/ethyl acetate, 2:1, *v*/*v*, R_f: 0.28) to yield **16** (101 mg, 0.28 mmol, 76 %) as yellow crystals, m.p. 202–204 °C; ^{1}H NMR (300 MHz, CD$_3$OD): δ = 1.46 (d, J = 6.6 Hz, 6 H, CH(CH$_3$)$_2$), 3.91 (s, 3 H, OCH$_3$), 4.67 (s, 1 H, NH), 4.79 (se, J = 6.6 Hz, 1 H, CH(CH$_3$)$_2$), 6.72 (dd, J = 3.6, 3.3 Hz, 1 H, arom), 7.12 (d, J = 8.7 Hz, 2 H, arom), 7.38 (d, J = 3.3 Hz, 1 H, arom), 7.81 (d, J = 9.0 Hz, 2 H, arom), 7.81 (d, J = 9.0 Hz, 1 H, arom), 7.89 (s, 1 H, arom), 8.08 (dd, J = 8.6, 2.0 Hz, 1 H, arom), 8.49 (d, J = 1.8 Hz, 1 H, arom); ^{13}C NMR (75 MHz, CD$_3$OD): δ = 22.7 (2 C), 43.9, 56.0, 113.2, 114.1, 115.5 (2 C), 115.6, 120.6, 128.4, 129.4 (2 C), 132.6, 133.4, 139.0, 146.0, 149.6, 154.5, 154.8, 160.5, 161.0, HR ESI-MS: calcd for $C_{22}H_{22}N_3O_2$: 360.17120 [M+H]$^+$, found: 360.17065.

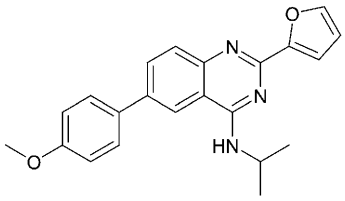

*3-(2-(Furan-2-yl)-4-(isopropylamino)quinazolin-6-yl)benzaldehyde (**17**)*: A solution of 2-(furan-2-yl)-6-iodo-*N*-isopropylquinazolin-4-amine (**10**; 115 mg, 0.30 mmol), 3-formylphenylboronic acid (48 mg, 0.32 mmol) and potassium carbonate (251 mg, 1.82 mmol) in dioxane/water (3.5 mL; 3:1, *v*/*v*) was degassed with ultrasound for 10 min. After addition of palladium acetate (1.4 mg, 6.06 μmol) the brown suspension was refluxed for 30 min (TLC control). After the suspension was cooled to room temperature, water (10 mL) was added and the suspension was extracted with ethyl acetate (3× 15 mL). The combined organic phases were washed with brine (10 mL) and dried over Na$_2$SO$_4$. After removing the solvent under reduced pressure the crude product was purified by column chromatography (*n*-hexane/ethyl acetate, 1:1, *v*/*v*, R_f: 0.39) to yield **17** (97 mg, 0.27 mmol, 90 %) as a light-green solid, m.p. 199–200 °C; ^{1}H NMR (300 MHz, CD$_3$OD): δ = 1.41 (d, J = 6.6 Hz, 6 H, CH(CH$_3$)$_2$), 4.71 (se, J = 6.6 Hz, 1 H, CH(CH$_3$)$_2$), 6.64 (dd, J = 2.1, 1.8 Hz, 1 H, arom), 7.29 (d, J = 3.3 Hz, 1 H, arom), 7.61 (t, J = 7.5 Hz, 1 H, arom),

 © 2009 Wiley-VCH Verlag GmbH & Co. KGaA, Weinheim

7.72 (s, 1 H, arom), 7.80 (d, $J=8.7$ Hz, 1 H, arom), 7.85 (d, $J=7.8$ Hz, 1 H, arom), 7.98 (dd, $J=8.9$, 2.2 Hz, 1 H, arom), 8.43 (d, $J=1.8$ Hz, 1 H, arom), 8.00 (d, $J=7.8$ Hz, 1 H, arom), 8.24 (s, 1 H, arom), 10.05 (s, 1 H, CHO); ^{13}C NMR (75 MHz, CD_3OD): $\delta=21.3$ (2 C), 42.9, 111.9, 113.2, 114.4, 120.4, 127.2, 128.0, 128.4, 129.6, 131.3, 132.7, 136.5, 137.4, 140.8, 144.7, 149.1, 153.2, 154.2, 159.5, 192.9; HR ESI-MS: calcd for $C_{22}H_{20}N_3O_2$: 358.15555 $[M+H]^+$, found: 358.15500.

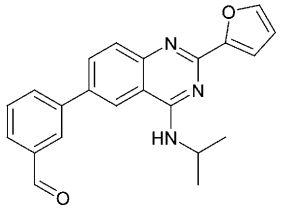

*6-(3-Aminophenyl)-2-(furan-2-yl)-***N***-isopropylquinazolin-4-amine (**26**)*: A solution of 2-(furan-2-yl)-6-iodo-*N*-isopropylquinazolin-4-amine (**10**; 500 mg, 1.32 mmol), 3-aminophenylboronic acid monohydrate (215 mg, 1.39 mmol) and caesium carbonate (2.15 g, 6.60 mmol) in dioxane/water (17 mL, 3:1, *v/v*) was degassed with ultrasound for 10 min. After addition of palladium acetate (5.9 mg, 26.4 μmol) the resulting black suspension was refluxed for 25 min (TLC control). After being cooled to room temperature, HCl (1 M; 25 mL) was added. The solution was extracted with dichloromethane (3× 30 mL). The combined organic phases were washed with brine (50 mL) and dried over Na_2SO_4. After the solvent was removed under reduced pressure the crude product was purified by column chromatography (*n*-hexane/ethyl acetate, 1:2, *v/v*, R_f: 0.30) to yield **26** (412 mg, 1.20 mmol, 91 %) as a light-yellow powder, m.p. 224–225 °C; ^{1}H NMR (300 MHz, CD_3OD): $\delta=1.41$ (d, $J=6.6$ Hz, 6 H, CH-$(CH_3)_2$), 4.75 (se, $J=6.6$ Hz, 1 H, $CH(CH_3)_2$), 6.64 (dd, $J=3.6$, 3.3 Hz, 1 H, arom), 6.77 (dd, $J=7.8$, 1.1 Hz, 1 H, arom), 7.11 (d, $J=7.8$ Hz, 1 H, arom), 7.13 (d, $J=1.2$ Hz, 1 H, arom), 7.23 (d, $J=7.5$ Hz, 1 H, arom), 7.33 (dd, $J=3.6$, 0.9 Hz, 1 H, arom), 7.75 (d, $J=1.8$ Hz, 1 H, arom), 7.83 (d, $J=8.7$ Hz, 1 H, arom), 7.98 (dd, $J=8.6$, 2.0 Hz, 1 H, arom), 8.39 (d, $J=1.5$ Hz, 1 H, arom); ^{13}C NMR (75 MHz, CD_3OD): $\delta=22.4$ (2 C), 43.9, 113.0, 114.1, 115.1, 115.5, 115.9, 118.1, 121.1, 127.9, 130.6, 132.9, 140.2, 142.2, 145.8, 149.3, 149.8, 154.5, 155.0, 160.0; HR ESI-MS: calcd for $C_{21}H_{21}N_4O$: 345.17154 $[M+H]^+$, found: 345.17099.

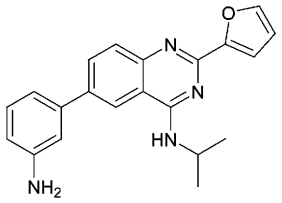

N-*(3-(2-(Furan-2-yl)-4-(isopropylamino)quinazolin-6-yl)phenyl)acetamide (**27**)*: A solution of 6-(3-aminophenyl)-2-(furan-2-yl)-*N*-isopropylquinazolin-4-amine (**26**; 35 mg, 0.10 mmol) and *N*-ethyldiisopropylamine (21 μL, 0.12 mmol) in THF (0.8 mL) was heated to 50 °C. After addition of acetyl chloride (7.6 μL, 0.11 mmol) the solution was stirred at this temperature for 3 h. After the solvent was removed under reduced pressure the crude product was purified by column chromatography (*n*-hexane/ethyl acetate, 1:4, *v/v*, R_f: 0.26) to yield **27** (29 mg, 0.08 mmol, 74 %) as a yellow solid, m.p. 180–182 °C; ^{1}H NMR (200 MHz, $CD_3OD/[D_6]DMSO$): $\delta=1.40$ (d, $J=6.2$ Hz, 6 H, $CH(CH_3)_2$), 2.17 (s, 3 H, $COCH_3$), 4.74 (se, $J=6.2$ Hz, 1 H, CH-$(CH_3)_2$), 6.67 (s, 1 H, arom), 7.33 (d, $J=3.0$ Hz, 1 H, arom), 7.46 (d, $J=7.8$ Hz, 1 H, arom), 7.55 (m, 2 H, arom), 7.78 (s, 1 H, arom), 7.80 (d, $J=8.8$ Hz, 1 H, arom), 8.00 (s, 1 H, arom), 8.02 (d, $J=7.8$ Hz, 1 H, arom), 8.46 (s, 1 H, arom); ^{13}C NMR (50 MHz, $CD_3OD/[D_6]DMSO$): $\delta=22.6$ (2 C), 24.2, 44.0, 113.2, 114.3, 115.5, 119.7, 120.3, 121.6, 123.9, 128.4, 130.5, 132.9, 139.2, 140.7, 141.9, 146.0, 150.1, 154.4, 155.2, 160.7, 171.4; HR ESI-MS: calcd for $C_{23}H_{23}N_4O_2$: 387.18210 $[M+H]^+$, found: 387.18110.

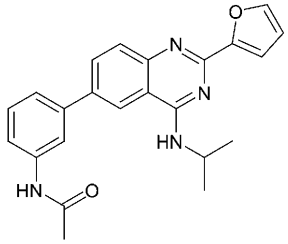

*2,2,2-Trichloro-*N*-(3-(2-(furan-2-yl)-4-(isopropylamino)quinazolin-6-yl)-phenyl)acetamide (**28**)*: A solution of 6-(3-aminophenyl)-2-(furan-2-yl)-*N*-isopropylquinazolin-4-amine (**26**; 70 mg, 0.20 mmol) and triethylamine (85 μL, 0.61 mmol) in THF (2.0 mL) was cooled to 0 °C. 2,2,2-Trichloroacetyl chloride (27 μL, 0.24 mmol) was added, which led to formation of a white precipitate. The suspension was stirred, overnight, at room temperature. After the solvent was removed under reduced pressure the crude product was purified by column chromatography (*n*-hexane/ethyl acetate, 1:1, *v/v*, R_f: 0.42) to yield **28** (81 mg, 0.17 mmol, 81 %) as a yellow solid, m.p. 220–222 °C; ^{1}H NMR (200 MHz, CD_3OD): $\delta=1.39$ (d, $J=6.2$ Hz, 6 H, $CH(CH_3)_2$), 4.75 (m, 1 H, $CH(CH_3)_2$,), 6.62 (d, $J=1.4$ Hz, 1 H, arom), 7.31 (d, $J=3.0$ Hz, 1 H, arom), 7.52 (d, $J=7.2$ Hz, 1 H, arom), 7.61 (m, 2 H, arom), 7.72 (s, 1 H, arom), 7.84 (d, $J=9.0$ Hz, 1 H, arom), 8.00 (s, 1 H, arom), 8.02 (d, $J=7.0$ Hz, 1 H, arom), 8.43 (s, 1 H, arom); ^{13}C NMR (100 MHz, $CD_3OD/[D_6]DMSO$): $\delta=22.6$ (2 C), 44.0, 94.5, 113.2, 114.4, 115.6, 121.5, 121.8, 122.0, 125.7, 128.6, 130.8, 132.9, 138.7, 139.1, 142.2, 146.1, 150.3, 154.4, 155.2, 160.6, 161.7; HR ESI-MS: calcd for $C_{23}H_{20}Cl_3N_4O_2$: 489.06518 $[M+H]^+$, found: 489.06464.

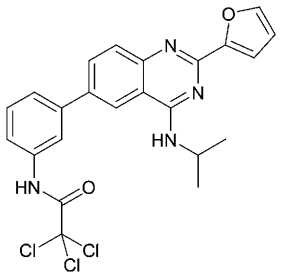

(E)*-4-(2-(Furan-2-yl)-4-(isopropylamino)quinazolin-6-yl)-2-methylbut-3-en-2-ol (**18**; TC-34)*: A solution of 6-(3-aminophenyl)-2-(furan-2-yl)-*N*-isopropylquinazolin-4-amine (**10**; 85 mg, 0.22 mmol), 2-methylbut-3-en-2-ol (70 μL, 0.67 mmol), tri-*o*-tolylphosphine (6.7 mg, 22.0 μmol), triethylamine (94 μL, 0.67 mmol) and palladium acetate (2.5 mg, 11.0 μmol) in acetonitrile (1.0 mL) was heated to 100 °C in a Pyrex® pressure tube. The yellow suspension turned to a black solution in 20 min. After 48 h the solvent was removed under reduced pressure and the crude product was purified by column chromatography (*n*-hexane/ethyl acetate, 1:3, *v/v*, R_f: 0.38) to yield

 © 2009 Wiley-VCH Verlag GmbH & Co. KGaA, Weinheim

18 (TC-34; 65 mg, 0.19 mmol, 86%) as a yellow solid, m.p. 144–146 °C; ^{1}H NMR (200 MHz, CD_3OD): δ = 1.39 (d, J = 7.4 Hz, 6H, CH-(CH_3)$_2$), 1.40 (s, 6H, C(CH_3)$_2$OH), 4.72 (se, J = 5.8 Hz, 1H, CH(CH_3)$_2$), 6.56 (d, J = 16.2 Hz, 1H, olefin), 6.60 (d, J = 3.0 Hz, 1H, arom), 6.72 (d, J = 16.2 Hz, 1H, olefin), 7.29 (d, J = 3.0 Hz, 1H, arom), 7.73 (s, 1H, arom), 7.88 (d, J = 8.8 Hz, 1H, arom), 8.22 (d, J = 9.0 Hz, 1H, arom), 8.53 (s, 1H, arom); ^{13}C NMR (50 MHz, CD_3OD): δ = 21.8 (2C), 29.2 (2C), 42.7, 69.8, 111.9, 112.4, 119.9, 120.4, 125.1, 128.4, 130.6, 134.9, 139.7, 144.4, 144.6, 150.0, 154.0, 159.0; HR ESI-MS: calcd for $C_{20}H_{24}N_3O_2$: 338.18685 [M+H]$^+$, found: 338.18630.

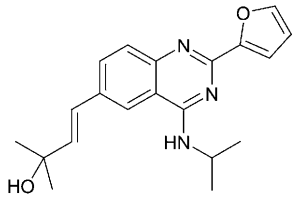

*(E)-tert-Butyl-3-(2-(furan-2-yl)-4-(isopropylamino)quinazolin-6-yl)acrylate (**19**)*: A solution of 6-(3-aminophenyl)-2-(furan-2-yl)-*N*-isopropylquinazolin-4-amine (**10**; 70 mg, 0.21 mmol), triethylamine (87 µL, 0.62 mmol), *tert*-butyl acrylate (90.2 µL, 0.62 mmol), tri-*o*-tolylphosphine (6.3 mg, 21.0 µmol) and palladium acetate (2.3 mg, 10.0 µmol) in acetonitrile (1.0 mL) was heated to 100 °C in a Pyrex® pressure tube for 72 h; the mixture turned to a dark-brown solution. After being cooled to room temperature the solution was poured in dichloromethane (25 mL). The organic phase was washed with water (15 mL) and brine (15 mL). After being dried over Na_2SO_4 the solvent was removed under reduced pressure. The crude product was purified by column chromatography (*n*-hexane/ethyl acetate, 3:1, *v/v*, R_f: 0.21) to yield **19** (44 mg, 0.13 mmol, 63%) as a yellow solid, m.p. 127–130 °C; ^{1}H NMR (200 MHz, CD_3OD/[D_6]DMSO): δ = 2.07 (d, J = 6.6 Hz, 6H, CH(CH_3)$_2$), 2.23 (s, 9H, C-(CH_3)$_3$), 5.40 (m, 1H, CH(CH_3)$_2$,), 7.29 (d, J = 15.8 Hz, 1H, olefin), 7.33 (s, 1H, arom), 8.01 (d, J = 3.0 Hz, 1H, arom), 8.36 (d, J = 16.2 Hz, 1H, olefin), 8.42 (d, J = 8.8 Hz, 1H, arom), 8.44 (s, 1H, arom), 8.64 (d, J = 7.8 Hz, 1H, arom), 9.09 (s, 1H, arom); ^{13}C NMR (75 MHz, CD_3OD/[D_6]DMSO): δ = 22.5 (2C), 28.5 (3C), 44.1, 81.7, 113.2, 114.8, 115.3, 121.5, 124.5, 128.4, 132.6, 133.0, 144.0, 146.2, 151.9, 154.2, 155.9, 160.6, 167.7; HR ESI-MS: calcd for $C_{22}H_{26}N_3O_3$: 380.19742 [M+H]$^+$, found: 380.19687.

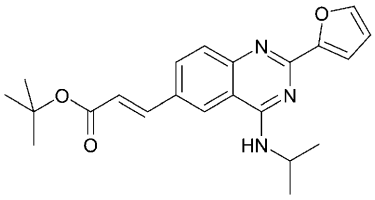

*3-(2-(Furan-2-yl)-4-(isopropylamino)quinazolin-6-yl)prop-2-yn-1-ol (**20**; TC-28)*: A mixture of DMF (2.0 mL) and triethylamine (0.8 mL, 10.8 mmol) was degassed with ultrasound for 45 min. After addition of 6-(3-aminophenyl)-2-(furan-2-yl)-*N*-isopropylquinazolin-4-amine (**10**; 120 mg, 0.32 mmol) and prop-2-yn-1-ol (92 µL, 1.58 mmol) the degassing was continued for 10 min. Afterwards bis(triphenylphosphine) palladium(II) dichloride (6.7 mg, 9.50 µmol), 1,1′-bis(diphenylphosphino)ferrocene (10.5 mg, 19.0 µmol), and copper(I) iodide (0.6 mg, 3.17 µmol) were added. The catalysts were dried before use. The solution was heated to 50 °C and stirred for 16 h at this temperature (TLC control). After being cooled to room temperature the solution was poured in ethyl acetate (10 mL). The organic phase was washed with diluted NH_4Cl (5 mL) solution and brine (5 mL). After being dried over Na_2SO_4 the solvent was removed at reduced pressure. The crude product was purified by column chromatography (*n*-hexane/ethyl acetate, 1:2, *v/v*, R_f: 0.35) to yield **20** (TC-28; 59 mg, 0.19 mmol, 61%) as a yellow solid, m.p. 199–200 °C; ^{1}H NMR: (300 MHz, CD_3OD): δ = 1.39 (d, J = 6.6 Hz, 6H, CH(CH_3)$_2$), 4.70 (se, J = 6.6 Hz, 1H, CH(CH_3)$_2$), 4.94 (s, 2H, CH_2OH), 6.67 (dd, J = 3.6 Hz, J = 3.3 Hz, 1H, arom), 7.34 (dd, J = 3.6, 0.9 Hz, 1H, arom), 7.76 (m, 3H, arom), 8.29 (s, 1H, arom); ^{13}C NMR (75 MHz, CD_3OD): δ = 22.3 (2C), 44.0, 51.2, 84.9, 89.9, 113.1, 114.7, 115.1, 121.2, 127.1, 127.8, 136.4, 146.1, 150.2, 154.2, 155.7, 160.1; HR ESI-MS: calcd for $C_{18}H_{18}N_3O_2$: 308.13990 [M+H]$^+$, found: 308.13935.

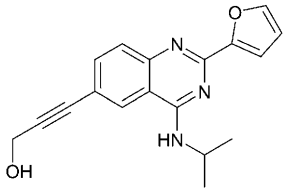

*2-(Furan-2-yl)-6-(4-methoxyphenyl)quinazolin-4(3H)-one (**11**)*: A solution of 2-(furan-2-yl)-6-iodoquinazolin-4(3*H*)-one (**5**; 3.00 g, 8.87 mmol), 4-methoxyphenylboronic acid (1.42 g, 9.32 mmol) and potassium carbonate (7.35 g, 53.2 mmol) in dioxane/water (100 mL, 3:1, *v/v*) was degassed with ultrasound for 10 min. After addition of palladium acetate (39.0 mg, 0.18 mmol) the solution was refluxed for 2 h (TLC control). After the solution was cooled to room temperature, HCl (1 M; 50 mL) was added, and the solution was extracted with ethyl acetate (3×100 mL). The combined organic phases were washed with brine (100 mL) and dried over Na_2SO_4. The solvent was removed under reduced pressure to yield **11** (1.76 g, 5.52 mmol, 62%) as a white solid. A small sample was purified by column chromatography (*n*-hexane/ethyl acetate, 1:2, *v/v*, R_f: 0.37) for analytical studies, m.p. 281–282 °C; ^{1}H NMR (200 MHz, [D_6]DMSO): δ = 3.78 (s, 3H, OCH_3), 6.73 (s, 1H, arom), 7.03 (d, J = 8.2 Hz, 2H, arom), 7.61 (d, J = 3.0 Hz, 1H, arom), 7.69 (d, J = 8.6 Hz, 2H, arom), 7.71 (s, 1H, arom), 8.03 (m, 2H, arom), 8.25 (s, 1H, arom), 12.5 (s, 1H, NH); ^{13}C NMR (50 MHz, [D_6]DMSO): δ = 55.9, 113.2, 115.1, 115.3 (2C), 122.1, 123.1, 128.6 (2C), 131.8, 133.3, 136.2, 138.5, 144.4, 146.8, 147.3, 148.1, 160.0, 162.3; HR ESI-MS: calcd for $C_{19}H_{15}N_2O_3$: 319.10827 [M+H]$^+$, found: 319.10772.

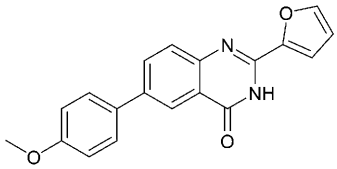

*4-Chloro-2-(furan-2-yl)-6-(4-methoxyphenyl)quinazoline (**12**)*: A solution of 2-(furan-2-yl)-6-(4-methoxyphenyl)quinazolin-4(3*H*)-one (**11**; 1.58 g, 4.96 mmol) in phosphoryl trichloride (25 mL) was refluxed for 3 h. Excess phosphoryl trichloride was removed under reduced pressure. The remaining solid was suspended in ethyl acetate (150 mL) and washed with NaOH (1 M; 3×150 mL). The combined organic phases were washed with brine (80 mL) and dried over

 © 2009 Wiley-VCH Verlag GmbH & Co. KGaA, Weinheim

Na_2SO_4. After removing the solvent under reduced pressure the crude product was purified by column chromatography (*n*-hexane/ethyl acetate, 3:1, *v*/*v*, R_f: 0.29) to yield **12** (0.75 g, 2.23 mmol, 45%) as a yellow solid, m.p. 158–160 °C; ^{1}H NMR (300 MHz, [D$_6$]DMSO): δ = 3.83 (s, 3H, OCH$_3$), 6.79 (d, J = 2.1 Hz, 1H, arom), 7.07 (d, J = 8.7 Hz, 2H, arom), 7.44 (d, J = 3.3 Hz, 1H, arom), 7.73 (d, J = 8.7 Hz, 2H, arom), 7.79 (d, J = 3.6 Hz, 1H, arom), 8.07 (d, J = 9.0 Hz, 1H, arom), 8.27 (dd, J = 9.0, 2.0 Hz, 1H, arom), 8.35 (d, J = 1.8 Hz, 1H, arom); ^{13}C NMR (50 MHz, [D$_6$]DMSO): δ = 112.7, 114.6 (2C), 114.7, 121.3, 127.1, 127.7 (2C), 128.4, 130.9, 138.0, 140.0, 146.6, 147.0, 150.0, 159.3, 159.8, 161.4; HR ESI-MS: calcd for $C_{19}H_{13}ClN_2O_2Na$: 359.05633 [M+Na]$^+$, found: 359.05578.

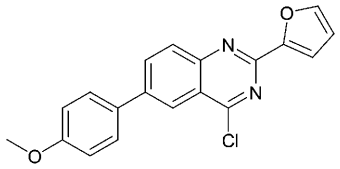

*2-(2-(Furan-2-yl)-6-(4-methoxyphenyl)quinazolin-4-ylamino)ethanol (**13**)*: A solution of 4-chloro-2-(furan-2-yl)-6-(4-methoxyphenyl)quinazoline (**12**; 65 mg, 0.19 mmol) and 2-aminoethanol (27 µL, 0.58 mmol) in propan-2-ol (3 mL) was refluxed for 30 min (TLC control). After the solution was cooled to room temperature the solvent was removed under reduced pressure. The crude product was purified by column chromatography (ethyl acetate, R_f: 0.38) to yield **13** (67 mg, 0.19 mmol, quant.) as a light-yellow crystalline solid, m.p. 188–190 °C; ^{1}H NMR: (200 MHz, [D$_6$]acetone): δ = 2.85 (m, 2H, H$_2$N–CH$_2$–CH$_2$OH), 3.81 (m, 2H, H$_2$N–CH$_2$–CH$_2$OH), 3.88 (s, 3H, OCH$_3$), 6.63 (dd, J = 3.4, 3.3 Hz, 1H, arom), 7.06 (d, J = 8.9 Hz, 2H, arom), 7.30 (d, J = 2.5 Hz, 1H, arom), 7.74 (d, J = 8.9 Hz, 2H, arom), 7.77 (d, J = 3.2 Hz, 1H, arom), 7.81 (d, J = 8.9 Hz, 1H, arom), 8.06 (dd, J = 8.5, 2.0 Hz, 1H, arom), 8.40 (d, J = 1.9 Hz, 1H, arom), NH, OH: not found; ^{13}C NMR (50 MHz, [D$_6$]acetone): δ = 45.1, 55.7, 62.0, 112.6, 113.1, 115.3 (2C), 115.5, 120.0, 129.0 (2C), 129.5, 132.2, 133.3, 138.6, 145.1, 150.3, 154.3, 154.9, 160.7, 161.3; HR ESI-MS: calcd for $C_{21}H_{20}N_3O_3$: 362.15047 [M+H]$^+$, found: 362.14992.

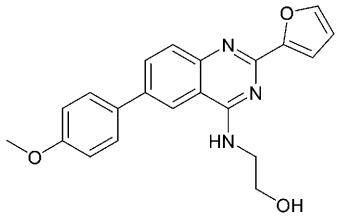

*(S)-Methyl 2-(2-(furan-2-yl)-6-(4-methoxyphenyl)quinazolin-4-ylamino)-3-hydroxypropanoate (**14**)*: A solution of 4-chloro-2-(furan-2-yl)-6-(4-methoxyphenyl)-quinazoline (**12**; 53 mg, 0.16 mmol), triethylamine (45 µL, 0.33 mmol) and L-serinmethylester hydrochloride (26 mg, 0.17 mmol) in THF (2.0 mL) was stirred at room temperature for 24 h (TLC control). The solvent was removed under reduced pressure. The crude product was purified by column chromatography (*n*-hexane/ethyl acetate, 1:4, *v*/*v*, R_f: 0.43) to yield **14** (44 mg, 0.11 mmol, 56%) as a yellow solid, m.p. 134–136 °C; ^{1}H NMR: (200 MHz, CD$_3$OD): δ = 3.75 (s, 3H, OCH$_3$), 4.11 (m, 2H, CH$_2$OH), 4.94 (t, J = 4.8 Hz, 1H, CH–CH$_2$OH), 4.88 (s, 3H, COOCH$_3$), 6.55 (d, J = 1.6 Hz, 1H, arom), 6.87 (d, J = 8.0 Hz, 2H, arom), 7.13 (d, J = 2.8 Hz, 1H, arom), 7.53 (d, J = 9.0 Hz, 2H, arom), 7.68 (s, 1H, arom), 7.70 (d, J = 8.8 Hz, 1H, arom), 7.87 (d, J = 8.8 Hz, 1H, arom), 8.16 (s, 1H, arom); ^{13}C NMR (50 MHz, CD$_3$OD): δ = 52.9, 55.8, 58.5, 62.6, 113.0, 114.5, 115.3, 115.4 (2C), 120.2, 128.3, 129.2 (2C), 133.1, 133.3, 139.7, 146.0, 149.5, 154.0, 154.1, 159.9, 161.1, 173.5; HR ESI-MS: calcd for $C_{23}H_{22}N_3O_5$: 420.15595 [M+H]$^+$, found: 420.15540.

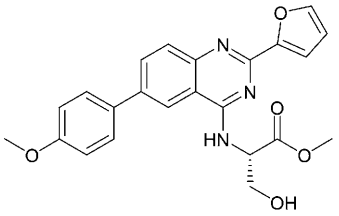

*3-(2-(Furan-2-yl)-6-(4-methoxyphenyl)quinazolin-4-yl)prop-2-yn-1-ol (**15**)*: A solution of 4-chloro-2-(furan-2-yl)-6-(4-methoxyphenyl)-quinazoline (**12**; 70 mg, 0.21 mmol), prop-2-yn-1-ol (60.7 µL, 1.04 mmol) and triethylamine (0.70 mL, 5.0 mmol) in DMF (1.5 mL) was degassed with ultrasound for 30 min. Afterwards palladium acetate (4.4 mg, 6.24 µmol) and copper(I) iodide (0.4 mg, 2.08 µmol) were added. The catalysts were dried before use. The solution was heated to 50 °C for 1 h and stirred at room temperature, overnight (TLC control). The resulting brown suspension was poured into ethyl acetate (30 mL) and washed with water (15 mL) and brine (15 mL). The combined aqueous phases were re-extracted with ethyl acetate (20 mL). After being dried over Na_2SO_4 the solvent was removed. The crude product was purified by column chromatography (*n*-hexane/ethyl acetate, 1:2, *v*/*v*, R_f: 0.42) to yield **15** (29 mg, 0.08 mmol, 39%) as a yellow solid, m.p. 218–219 °C; ^{1}H NMR (300 MHz, CDCl$_3$): δ = 3.89 (s, 3H, OCH$_3$), 4.35 (s, 1H, OH), 4.72 (s, 2H, CH$_2$OH), 6.62 (dd, J = 3.6, 3.3 Hz, 1H, arom), 7.06 (d, J = 9.0 Hz, 2H, arom), 7.48 (d, J = 3.3 Hz, 1H, arom), 7.67 (d, J = 9.3 Hz, 2H, arom), 7.69 (s, 1H, arom), 8.13 (m, 2H, arom), 8.33 (s, 1H, arom); ^{13}C NMR (50 MHz, [D$_6$]acetone): δ = 50.9, 56.3 80.5, 81.1, 113.7, 115.2, 116.0 (2C), 123.7, 125.0, 129.5, 129.8 (2C), 130.3, 132.6, 135.4, 147.4, 150.9, 153.6, 153.8 154.6, 161.4; HR ESI-MS: calcd for $C_{22}H_{17}N_2O_3$: 357.12392 [M+H]$^+$, found: 357.12337.

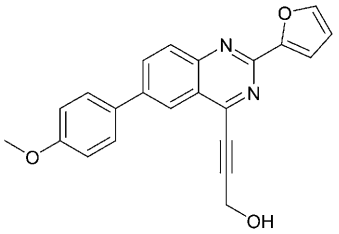

*6-Iodoquinazolin-4(3H)-one (**4**)*: A mixture of 2-amino-5-iodobenzoic acid (**3**; 5.0 g, 19.0 mmol) and formamidine hydrochloride (2.3 g, 28.5 mmol) was grounded and heated to 210 °C for 20 min. The resulting solid was suspended in NaOH (0.3 M, 65 mL) and treated with ultrasound. The product was filtered, washed with water and dried under vacuum to yield **4** (4.42 g, 16.3 mmol, 86%) as a gray solid, m.p. 264 °C; ^{1}H NMR (300 MHz, [D$_6$]DMSO): δ = 7.47 (d, J = 8.7 Hz, 1H, arom), 8.11 (dd, J = 8.7, 2.2 Hz, 1H, arom), 8.15 (s, 1H, arom), 8.40 (d, J = 1.8 Hz, 1H, arom), 12.43 (s, 1H, NH); the analytical data are in agreement with ref. [35].

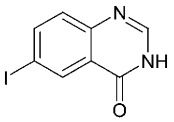

 © 2009 Wiley-VCH Verlag GmbH & Co. KGaA, Weinheim

*4-Chloro-6-iodoquinazoline (**6**)*: A solution of 6-iodoquinazolin-4(3*H*)-one (**4**; 4.42 g, 16.3 mmol) and a drop of DMF in thionyl chloride (50 mL) was refluxed for 4 h. The resulting solid was suspended in ethyl acetate (400 mL) and washed with NaOH (1 M; 3×400 mL). The organic phase was washed with brine (200 mL) and dried over Na_2SO_4. The solvent was removed under reduced pressure. The crude product was purified by column chromatography (*n*-hexane/ethyl acetate, 3:1, *v/v*, R_f: 0.44) to yield **6** (3.15 g, 10.9 mmol, 66%) as a yellow solid, m.p. 173–175 °C; ^{1}H NMR (300 MHz, [D$_6$]DMSO): δ = 7.61 (d, *J* = 8.4 Hz, 1 H, arom), 8.22 (dd, *J* = 8.4, 1.8 Hz, 1 H, arom), 8.43 (d, *J* = 1.8 Hz, 1 H, arom), 8.69 (s, 1 H, arom). The analytical data are in agreement with the literature.[36]

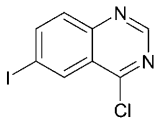

*6-Iodo-*N*-isopropylquinazolin-4-amine (**8**)*: A solution of 4-chloro-6-iodoquinazoline (**6**; 200 mg, 0.69 mmol) and isopropylamine (0.15 mL, 1.72 mmol) in propan-2-ol (10 mL) was stirred at 60 °C for 4 h (TLC control). The solvent was removed under reduced pressure. The crude product was purified by column chromatography (*n*-hexane/ethyl acetate, 1:3, *v/v*, R_f: 0.34) to yield **8** (215 mg, 0.69 mmol, quant.) as white crystals, m.p. 184–186 °C; ^{1}H NMR (200 MHz, CD$_3$OD): δ = 1.29 (d, *J* = 6.2 Hz, 6 H, CH(CH$_3$)$_2$), 4.50 (se, *J* = 6.4 Hz, 1 H, CH(CH$_3$)$_2$), 7.36 (d, *J* = 8.8 Hz, 1 H, arom),7.95 (d, *J* = 8.8 Hz, 1 H, arom), 8.39 (s, 1 H, arom), 8.57 (s, 1 H, arom); ^{13}C NMR (50 MHz, CD$_3$OD): δ = 22.2 (2 C), 44.1, 90.8, 118.2, 129.4, 132.8, 142.7, 148.9, 156.5, 159.3; HR ESI-MS: calcd for $C_{11}H_{13}IN_3$: 314.01542 [*M*+H]$^+$, found: 314.01483.

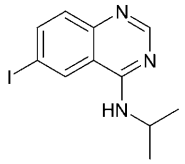

N-*Isopropyl-6-(4-methoxyphenyl)quinazolin-4-amine (**21**)*: A solution of 6-iodo-*N*-isopropylquinazolin-4-amine (**8**; 100 mg, 0.32 mmol), 4-methoxyphenylboronic acid (51 mg, 0.34 mmol) and potassium carbonate (265 mg, 1.92 mmol) in dioxane/water (3.7 mL, 3:1, *v/v*) was degassed with ultrasound for 10 min. After addition of palladium acetate (0.7 mg, 3.19 μmol) the solution was refluxed for 2 h (TLC control). After the solution was cooled to room temperature, HCl (1 M; 10 mL) was added and the solution was extracted with dichloromethane (3×20 mL). The combined organic phases were washed with brine (30 mL) and dried over Na_2SO_4. The solvent was removed under reduced pressure. The crude product was purified by column chromatography (ethyl acetate, R_f: 0.16) to yield **21** (76 mg, 0.26 mmol, 81%) as a white crystalline solid, m.p. 186–187 °C; ^{1}H NMR (300 MHz, CD$_3$OD): δ = 1.40 (d, *J* = 6.6 Hz, 6 H, CH(CH$_3$)$_2$), 3.89 (s, 3 H, OCH$_3$), 4.62 (se, *J* = 6.6 Hz, 1 H, CH(CH$_3$)$_2$, 7.07 (d, *J* = 8.7 Hz, 2 H, arom), 7.75 (d, *J* = 8.7 Hz, 2 H, arom), 7.76 (d, *J* = 8.7 Hz, 1 H, arom), 8.06 (dd, *J* = 8.7, 1.5 Hz, 1 H, arom), 8.44 (d, *J* = 1.5 Hz, 1 H, arom), 8.43 (s, 1 H, arom); ^{13}C NMR (75 MHz, CD$_3$OD): δ = 22.4 (2 C), 44.1, 55.8, 115.4 (2 C) 116.7, 120.5, 128.0, 129.4 (2 C), 132.8, 133.5, 140.2, 148.5, 155.6, 160.7, 161.2; HR ESI-MS: calcd for $C_{18}H_{20}N_3O$: 294.16064 [*M*+H]$^+$, found: 294.16009.

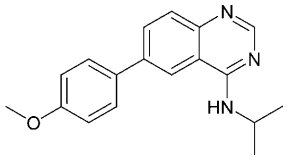

N-*(3-Fluorophenyl)-6-iodoquinazolin-4-amine (**9**)*: A solution of 4-chloro-6-iodoquinazolin (**6**; 1.50 g, 5.20 mmol), 3-fluoroaniline (1.22 g, 11.4 mmol) and a drop of concentrated HCl in propan-2-ol (70 mL) was refluxed for 30 min (TLC control). The solvent was removed under reduced pressure and the remaining solid dissolved in ethyl acetate (300 mL). The solution was washed with NaOH (1 M, 3×150 mL). Afterwards the organic phase was washed with brine (150 mL) and dried over Na_2SO_4. The crude product was purified by column chromatography (*n*-hexane/ethyl acetate, 3:1, *v/v*, R_f: 0.18) to yield **9** (1.71 g, 4.7 mmol, 90%) as a yellow solid, m.p. 202–204 °C; ^{1}H NMR (200 MHz, [D$_6$]DMSO): δ = 6.97 (td, *J* = 7.7, 1.8 Hz, 1 H, arom), 7.43 (q, *J* = 7.5 Hz, 1 H, arom), 7.58 (d, *J* = 8.8 Hz, 1 H, arom), 7.70 (d, *J* = 8.1 Hz, 1 H, arom), 7.95 (dt, *J* = 12.1, 2.2 Hz, 1 H, arom), 8.13 (dd, *J* = 8.7, 1.8 Hz, 1 H, arom), 8.69 (s, 1 H, arom), 9.01 (d, *J* = 1.7 Hz, 1 H, arom), 9.96 (s, 1 H, NH); ^{13}C NMR (50 MHz, [D$_6$]DMSO): δ = 91.7, 108.6 (d, *J* = 25.9 Hz), 110.0 (d, *J* = 21.0 Hz), 116.8, 117.5 (d, *J* = 2.7 Hz), 129.8, 129.9 (d, *J* = 10.1 Hz), 131.3, 140.8, 141.4, 148.7, 154.5, 156.2, 161.9 (d, *J* = 240.0 Hz); HR ESI-MS: calcd for $C_{14}H_{10}FIN_3$: 365.98979 [*M*+H]$^+$, found: 365.98944.

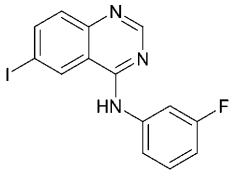

N-*(3-Fluorophenyl)-6-(4-methoxyphenyl)quinazolin-4-amine (**22**)*: A solution of *N*-(3-fluorophenyl)-6-iodoquinazolin-4-amine **9** (150 mg, 0.41 mmol), 4-methoxyphenylboronic acid (65.5 mg, 0.43 mmol), caesium carbonate (670 mg, 2.05 mmol) and palladium acetate (1.84 mg, 8.2 μmol) in dioxane/water (4.7 mL, 3:1, *v/v*) was refluxed for 30 min (TLC control). After being cooled to room temperature the solution was diluted with water (10 mL) and extracted with ethyl acetate (3×10 mL). The combined organic phases were washed with brine (10 mL) and dried over Na_2SO_4. The solvent was removed under reduced pressure. The crude product was purified by column chromatography (*n*-hexane/ethyl acetate, 1:3, *v/v*, R_f: 0.53) to yield **22** (126 mg, 0.37 mmol, 89%) as a yellow solid, m.p. 213–215 °C; ^{1}H NMR (400 MHz, CD$_3$OD/[D$_6$]DMSO): δ = 3.76 (s, 3 H, OCH$_3$), 6.13 (td, *J* = 8.0, 2.0 Hz, 1 H, arom), 6.45 (d, *J* = 8.8 Hz, 1 H, arom), 6.62 (q, *J* = 8.4 Hz, 1 H, arom), 6.87 (d, *J* = 8.0 Hz, 1 H, arom), 7.01 (d, *J* = 8.8 Hz, 1 H, arom), 7.06 (d, *J* = 8.8 Hz, 1 H, arom), 7.12 (d, *J* = 11.6 Hz, 1 H, arom), 7.35 (dd, *J* = 8.8, 2.0 Hz, 1 H, arom), 7.82 (s, 1 H, arom), 7.87 (d, *J* = 1.6 Hz, 1 H, arom); ^{13}C NMR (100 MHz, CD$_3$OD/[D$_6$]DMSO): δ = 55.7, 110.2 (d, *J* = 25.7 Hz), 111.3 (d, *J* = 21.2 Hz), 115.3 (2 C), 116.6, 118.8 (d, *J* = 2.9 Hz), 120.2, 128.6, 129.4 (2 C), 130.7 (d, *J* = 9.5 Hz), 132.9, 133.0, 140.2, 141.2 (d, *J* = 11.0 Hz), 149.2, 154.9, 159.2, 160.9, 163.7 (d, *J* = 241.1 Hz); HR ESI-MS: calcd for $C_{21}H_{17}FN_3O$: 346.13557 [*M*+H]$^+$, found: 346.13486.

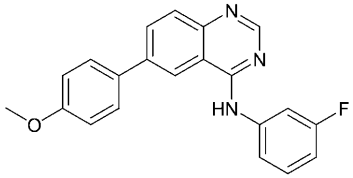

*6-(3-Aminophenyl)-*N*-(3-fluorophenyl)quinazolin-4-amine (**23**)*: A solution of *N*-(3-fluorophenyl)-6-iodoquinazolin-4-amine (**9**; 150 mg, 0.41 mmol), 3-aminophenylboronic acid monohydrate (66.8 mg, 0.43 mmol), caesium carbonate (670 mg, 2.05 mmol) and palladium acetate (1.84 mg, 8.2 μmol) in dioxane/water (4.7 mL, 3:1, *v/v*) was refluxed for 30 min (TLC control). After being cooled to room tem-

 © 2009 Wiley-VCH Verlag GmbH & Co. KGaA, Weinheim

perature the solution was diluted with water (10 mL) and extracted with ethyl acetate (3×10 mL). The combined organic phases were washed with brine (10 mL) and dried over Na_2SO_4. The solvent was removed under reduced pressure. The crude product was purified by column chromatography (*n*-hexane/ethyl acetate, 1:3, *v*/*v*, R_f: 0.30) to yield **23** (0.137 g, 0.39 mol, 96%) as a yellow solid, m.p. 221–223 °C; ^{1}H NMR (200 MHz, [D$_6$]DMSO): δ=5.21 (br, 2H, NH_2), 6.61 (d, J=8.4 Hz, 1H, arom), 6.92 (m, 3H, arom), 7.16 (dd, J=8.0, 7.8 Hz, 1H, arom), 7.40 (q, J=8.4 Hz, 1H, arom), 7.67 (d, J=8.2 Hz, 1H, arom), 7.83 (d, J=8.8 Hz, 1H, arom), 7.93 (dt, J=12.0, 2.2 Hz, 1H, arom), 8.03 (dd, J=8.4, 1.2 Hz, 1H, arom), 8.62 (s, 1H, arom), 8.72 (s, 1H, arom), 10.01 (s, 1H, NH); ^{13}C NMR (75 MHz, [D$_6$]DMSO): δ=108.8 (d, J=25.9 Hz), 109.9 (d, J=21.1 Hz), 112.6, 113.6, 114.9, 115.3, 117.7 (d, J=2.7 Hz), 120.1, 128.3, 129.5, 129.9 (d, J=9.4 Hz), 131.9, 139.4, 139.9, 141.1 (d, J=11.4 Hz), 148.9, 149.2, 154.0, 157.6, 161.9 (d, J=240.9 Hz); HR ESI-MS: $[M+H]^+$ calcd for $C_{20}H_{16}FN_4$: 331.13590, found: 331.13504.

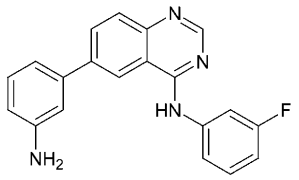

(E)*-4-(4-(3-Fluorophenylamino)quinazolin-6-yl)-2-methylbut-3-en-2-ol* (***24***): A solution of *N*-(3-fluorophenyl)-6-iodoquinazolin-4-amine (**9**; 200 mg, 0.55 mmol), 2-methylbut-3-en-2-ol (167 µL, 0.67 mmol), tri-*o*-tolylphosphine (16.7 mg, 54.0 µmol), triethylamine (0.30 mL, 4.08 mmol) and palladium acetate (6.1 mg, 27.0 µmol) in acetonitrile (1.5 mL) was heated to 100 °C in a Pyrex® pressure tube. After 18 h the solution was poured into dichloromethane (50 mL) and washed with water (30 mL) and brine (30 mL). After being dried over Na_2SO_4 the solvent was removed under reduced pressure. The crude product was purified by column chromatography (*n*-hexane/ethyl acetate, 1:3, *v*/*v*, R_f: 0.27) to yield **24** (129 mg, 0.40 mmol, 73%) as a yellow solid, m.p. 184–186 °C; ^{1}H NMR (400 MHz, CD_3OD): δ=1.34 (s, 6H, $C(CH_3)_2$), 6.67 (d, J=16.1 Hz, 1H, olefin), 6.73 (d, J=16.1 Hz, 1H, olefin), 6.95 (td, J=8.4, 2.3 Hz, 1H, arom), 7.43 (q, J=8.1 Hz, 1H, arom), 7.41 (d, J=8.1 Hz, 1H, arom), 7.45 (d, J=8.7 Hz, 1H, arom), 7.98 (m, 2H, arom), 8.54 (s, 1H, arom), 8.62 (s, 1H, arom), 9.85 (s, 1H, NH); ^{13}C NMR (100 MHz, [D$_6$]DMSO): δ=30.1 (2C), 69.4, 108.6 (d, J=26.0 Hz), 109.8 (d, J=21.0 Hz), 115.3, 117.5, 119.9, 124.3, 128.1, 129.9 (d, J=9.0 Hz), 131.0, 135.4, 141.0, 141.2, 149.1, 153.8, 157.3, 161.9 (d, J=241.0 Hz); HR ESI-MS: calcd for $C_{19}H_{19}FN_3O$: 324.15122 $[M+H]^+$, found: 324.15055.

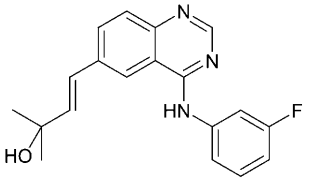

3-(4-(3-Fluorophenylamino)quinazolin-6-yl)prop-2-yn-1-ol (***25***; *TC-107*): A solution of *N*-(3-fluorophenyl)-6-iodoquinazolin-4-amine (**9**; 240 mg, 0.66 mmol), prop-2-yn-1-ol (192 µL, 3.29 mmol), palladium acetate trimer (4.4 mg, 6.57 µmol), 1,1′-bis(diphenylphosphino)ferrocene (21.8 mg, 39.4 µmol) and copper(I) iodide (1.2 mg, 6.57 µmol) in triethyl amine (1.0 mL, 7.20 mmol) and DMF (3.0 mL) was heated to 50 °C for 18 h. After being cooled to room temperature the solution was poured into ethyl acetate (10 mL) and washed with saturated NH_4Cl (7 mL), water (7 mL) and brine (7 mL). After being dried over Na_2SO_4 the solvent was removed under reduced pressure. The crude product was purified by column chromatography (*n*-hexane/ethyl acetate, 1:3, *v*/*v*, R_f: 0.34) to yield **25** (TC-107, 180 mg, 0.61 mmol, 93%) as a yellow solid, m.p. 218–220 °C; ^{1}H NMR (300 MHz, CD_3OD): δ=4.45 (s, 2H, CH_2OH), 6.89 (tdd, J=8.4, 2.7, 0.9 Hz, 1H, arom), 7.37 (qd, J=8.4, 1.8 Hz, 1H, arom), 7.56 (dd, J=8.1, 1.2 Hz, 1H, arom), 7.76 (d, J=11.4 Hz, 1H, arom), 7.81 (m, 2H, arom), 8.50 (d, J=1.5 Hz, 1H, arom), 8.57 (s, 1H, arom); ^{13}C NMR (75 MHz, CD_3OD): δ=51.2, 84.5, 90.8, 110.7 (d, J=26.6 Hz), 111.9 (d, J=21.6 Hz), 116.6, 119.1 (d, J=2.8 Hz), 123.0, 127.0, 128.4, 131.0 (d, J=9.4 Hz), 136.8, 141.7 (d, J=10.5 Hz), 149.9, 156.1, 159.2, 164.2 (d, J=242.1 Hz); HR ESI-MS: calcd for $C_{17}H_{13}FN_3O$: 294.10427 $[M+H]^+$, found: 294.10368.

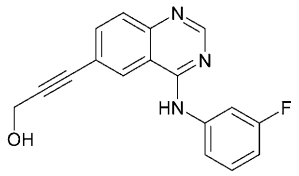

Cell culture and compound treatment (HeLa and RPE cells): Adherent HeLa cells were routinely passaged and maintained in DMEM medium supplemented with fetal bovine serum (FBS; 10%), penicillin/streptomycin (1%) and L-glutamine (2 mM). The cells were incubated at 37 °C, in a humidified atmosphere with CO_2 (5%). The hTERT-RPE1 cells were grown in DMEM with FBS (10%). HeLa cells constitutively expressing green fluorescent protein (GFP)-conjugated histone H2B and mRed fluorescent protein (mRFP)-conjugated α-tubulin[37] were maintained in DMEM medium supplemented with FBS (10%), penicillin/streptomycin (1%), L-glutamine (2 mM) and puromycin (0.5 µg mL^{-1}) and incubated at 37 °C, in a humidified atmosphere with CO_2 (5%). Compounds TC-28, TC-34, TC-107 and ZM1 were resuspended in DMSO (20 mM stocks) and added to the cell culture medium at the final concentrations indicated in the text.

For Western blot analysis of HH3 phosphorylation levels in mitosis HeLa cells were arrested with thymidine (2 mM) for 18 h, released into fresh medium for 6 h, and blocked with nocodazole (2 µM) for 16 h. DMSO or the different compounds were added 1 h after thymidine release. Mitotic cells were shaken off and lysed in Tris pH 6.8 (50 mM) with SDS (2%). Samples were sonicated and boiled. The protein extract (30 µg; as determined by using the Bradford assay, Bio-Rad) was loaded on SDS-PAGE, transferred to a nitrocellulose membrane and probed with anti-phospho-HH3 (Upstate), anti-AurA[38] and anti-tubulin antibodies (Sigma, DM1A).

Treatment of cells and analysis of phenotypes: For live cell analysis, H2B–GFP/mRFP–α-tubulin expressing HeLa cells were treated with DMSO or ZM1 (2 µM) or TC-28, TC-34 or TC-107 (40 µM). Upon treatment, living cells were added to a humidified chamber at 37 °C with CO_2 (5%) attached to a Carl Zeiss microscope (SN:3834000366) equipped with a Hamamatsu EM-CCD digital camera, controlled by AxioVision 4.6 software. Cells were imaged every 3 or 4.5 min (depending on the number of fields filmed) for over 16–24 h. Images were taken with the AxioCam MRm 426205 objective and processed by using AxioVision software.

 © 2009 Wiley-VCH Verlag GmbH & Co. KGaA, Weinheim

For fixed cell analysis, HeLa or H2B–GFP/mRFP–α-tubulin expressing HeLa cells were grown on glass cover-slips and treated as described above. Cells were fixed in ice cold methanol and mounted in Mowiol. Alternatively, nonfluorescent HeLa cells were treated and subjected to immunofluorescence by using anti-tubulin antibodies (Sigma, DM1A) and Hoechst 33342 to stain the DNA. Cells were observed by using a Leica DMI6000B microscope with the HCXPL APOCS 63× 1.4 objective. Images were taken with a Leica DFC 350FX camera, controlled by Leica Application Suit (LAS-AF 6000) software and processed with Adobe Photoshop.

Fluorescence activated cell sorting (FACS): After treatment, FACS analysis was performed by using a BD FACSCanto™ Flow Cytometer (Cat. No. 335860, BD Biosciences) by using FACSDiva Software. Cells were trypsinized, washed wish PBS and fixed, overnight, in EtOH (−20 °C). After being washed with PBS, cells were stained with a propidium iodide (PI; 15 μg mL^{-1})/RNase A (30 μg mL^{-1}) solution for 30 min at 37 °C. RNase was added to avoid signals caused by the binding of PI to RNA.

In vitro kinase assay: The IC_{50} for the different compounds was determined with Invitrogen Z′-LYTE kinase assay kit Ser/Thr 1 peptide PV3174 by following the manufacturer's instructions. In brief, the concentrations of the kinases at the reported $K_{M\,app}$ ATP concentrations (AurA: 10 μm ATP, AurB: 64 μm ATP) were first optimized by using ten-point dose-response curves; this gave a protein concentration that resulted in approximately 30% phosphorylation. This amount was then used in subsequent assay steps. Compounds were prepared in 384-well plates (Greiner 384-well PP 781280) at the highest concentration of 400 μm (in 4% DMSO) and then serially diluted in twofold steps manually, and the DMSO percentage was kept constant. Compound solution (1.25 μL) was subsequently transferred 1:1 to a 384-well assay plate (Greiner 384-well ProxiPlate Plus F 6008 260) for screening at a highest concentration in the final assay of 100 μm (in 1% DMSO). In the first step, a solution containing AurA (2.5 μL, 8 nm; batch S74, prepared in-house at EMBL) or aurora B (40 nm; Invitrogen PV3970) and Ser/Thr peptide 1 (4 μm; Invitrogen PV3174) was added to each well, followed by the ATP solution (1.25 μL; 40 μm for AurA, 256 μm for AurB). The final reaction volume (5 μL) consisted of AurA (4 nm) or AurB (20 nm), Ser/Thr 1 peptide (2 μm), HEPES pH 7.5 (50 mm), BRIJ-35 (0.01%), $MgCl_2$ (10 mm) and EGTA (1 mm), in addition to ATP (10 μm or 64 μm for AurA and AurB, respectively). To simulate 100% inhibition (positive control), buffer was added instead of the ATP solution, while in the 0% inhibition wells compound was replaced by DMSO solution (4%). The plates were then centrifuged at 1100 *g* for 1 min, followed by incubation at room temperature for 1 h. In the second step, development solution (2.5 μL; development A reagent diluted 1:2048 in development buffer) was added to each well, followed again by centrifugation at 1100 *g* for 1 min and subsequent incubation at room temperature for 1 h. In the final step, the reaction in each well was stopped by the addition of stop reagent (2.5 μL), followed by a brief centrifugation step and immediate readout (PerkinElmer EnVision HTS; excitation 405 nm, coumarin emission 450 nm, fluorescein emission 535 nm). Percentage phosphorylation was calculated by using 0 and 100% phosphorylation controls. The former wells contained DMSO (1.25 μL, 4%), buffer (1.25 μL, as above) and Ser/Thr 1 peptide solution (2.5 μL, 4 μm; without kinase), while in the latter the peptide solution was replaced by a solution of a supplied phosphopeptide (4 μm). The action of the development reagent was assessed by using protease controls (standard wells with and without development solution added in step two). The [coumarin emission/fluorescein emission] ratio was used together with the minimum and maximum signals at the two wavelengths to yield percentage phosphorylation, from which inhibition was derived (according to the manufacturer's instructions). Calculated inhibition values were then fitted to 11-point variable slope sigmoidal dose-response curves by using GraphPad Prism software, to yield the compound IC_{50} values.

To determine the IC_{50} of receptor tyrosine kinase, an assay based on the ELISA principle with kinases from Biomol (N-terminally fused to GST), POD-coupled antibody from Calbiochem (PY20) and BM chemiluminescence ELISA substrate from Roche was performed.

In short, a white 96-well microplate was incubated, overnight, with 100 μL per well of the substrate solution (poly-Glu-Tyr diluted with PBS to 100 μg mL^{-1}) at 4 °C. The solution was removed and the plate was washed twice for 2 min with PBS-T. Afterwards the kinase solution (50 μL per well; KDR (VEGFR2), 5 ng; Flt4 (VEGFR3), 20 ng; EGFR, 5 ng; IGFR, 15 ng; FGFR, 10 ng and Tie2, 20 ng) and the inhibitor solution (25 μL per well) were added to each well. To obtain the positive and negative controls, aqueous DMSO (5%; 25 μL per well) were used instead of inhibitor solution. Addition of ATP solution (25 μL per well) started the reaction; $MnCl_2$ solution (40 mm; 25 μL per well) was added to the negative control instead of ATP. After incubation under mild shaking conditions for 30 min at room temperature the plate was washed with PBS-T (3×2 min) and subsequently incubated with antibody solution (anti-phosphotyrosine antibody (POD-coupled) diluted 1:10 000 in PBS-T+BSA (0.2%, *m/v*; 100 μL per well) for 1 h again while being shaken. Finally, the plate was washed with PBS-T (3×5 min) and supplemented with the chemiluminescence substrate (50 μL per well). After 3 min the emitted luminescence was measured by using a luminometer. A positive control was measured without inhibitor to determine the activity of the kinase, a negative control without inhibitor and ATP was used to abstract the background signal from the results. For determination of IC_{50} values, the relative luminescence units per second (RLU/s) were plotted against the inhibitor concentrations. In doing so each concentration measurement was performed in triplicate and at least five different inhibitor concentrations were used to determine the IC_{50} value.

Cilia assembly and disassembly assays: Cilia assembly and disassembly assays were performed as described by Pugacheva et al.[4] Briefly, to study cilia assembly hTRET-RPE1 cells were plated at 30% confluence in plates containing glass cover-slips, and starved for 48 h (in Opti-MEM) to induce cilia formation in the presence of ZM1, TC-28 or DMSO (vehicle). For analysis of cilia disassembly, cilia were assembled by 48 h starvation in Opti-MEM, and disassembled by incubation in DMEM with FBS (10%). Cells were fixed after 2 and 4 h. ZM1, TC-28 or DMSO (vehicle) were added to hTERT-RPE1 cells 2 h prior to the initiation of cilia disassembly. To visualize the centrosomes and cilia, fixed cells were immunostained with anti-γ-tubulin (Sigma, GTU88) and anti-acetylated tubulin (Sigma); DNA was stained with Hoechst 33342.

Acknowledgements

H2B–GFP/mRFP–α-tubulin expressing HeLa cells were a kind gift from Patrick Meraldi (ETH, Zurich, Switzerland). We thank Eveline Boerthout for participating in the preliminary experiments and David Vanneste for help with cell culture handling. We thank Luis Serrano for the manual docking of TC-28. We thank the Volkswagen Foundation for financial support.

 © 2009 Wiley-VCH Verlag GmbH & Co. KGaA, Weinheim

Keywords: antitumor agents · biological activity · cell cycle · inhibitors · kinases

[1] B. A. Weaver, D. W. Cleveland, *Cancer Res.* **2007**, *67*, 10103–10105.
[2] E. A. Nigg, *Nat. Rev. Mol. Cell Biol.* **2001**, *2*, 21–32.
[3] R. Crane, B. Gadea, L. Littlepage, H. Wu, J. V. Ruderman, *Biol. Cell* **2004**, *96*, 215–229.
[4] E. N. Pugacheva, S. A. Jablonski, T. R. Hartman, E. P. Henske, E. A. Golemis, *Cell* **2007**, *129*, 1351–1363.
[5] D. Mahadevan, S. Beeck, *Expert Opin. Drug Discovery* **2007**, *2*, 1011–1026.
[6] N. Keen, S. Taylor, *Nat. Rev. Cancer* **2004**, *4*, 927–936.
[7] R. Carvajal, A. Tse, G. Schwartz, *Clin. Cancer Res.* **2006**, *12*, 6869–6875.
[8] S. Anand, S. Penrhyn-Lowe, A. R. Venkitaraman, *Cancer Cell* **2003**, *3*, 51–62.
[9] B. T. McGrogan, B. Gilmartin, D. N. Carney, A. McCann, *Biochim. Biophys. Acta, Rev. Cancer* **2008**, *1785*, 96–132.
[10] S. Taylor, J. M. Peters, *Curr. Opin. Cell Biol.* **2008**, *20*, 77–84.
[11] T. V. Hughes, S. L. Emmanuel, H. R. O'Grady, P. J. Connolly, *Bioorg. Med. Chem. Lett.* **2008**, *18*, 5130–5133.
[12] J. D. Oslob, M. J. Romanowski, D. A. Allen, S. Baskaran, M. Bui, R. A. Elling, *Bioorg. Med. Chem. Lett.* **2008**, *18*, 4880–4884.
[13] K. Hoar, A. Chakravarty, C. Rabino, D. Wysong, D. Bowman, *Mol. Cell. Biol.* **2007**, *27*, 4513–4525.
[14] M. G. Manfredi, J. A. Ecsedy, K. A. Meetze, S. K. Balani, O. Burenkova, *Proc. Natl. Acad. Sci. USA* **2007**, *104*, 4106–4111.
[15] Y. G. Lin, A. Immaneni, W. M. Merrit, L. S. Mangala, S. W. Kin, *Clin. Cancer Res.* **2008**, *14*, 5437–5446.
[16] J. Yang, T. Ikezoe, C. Nishioka, T. Tasaka, A. Taniguchi, Y. Kuwayama, *Blood* **2007**, *110*, 2034–2040.
[17] G. de Carcer, I. Perez de Castro, M. Malumbres, *Curr. Med. Chem.* **2007**, *14*, 969–985.
[18] D. W. Sherbenou, M. J. Wong, A. Humayun, L. S. McGreevey, P. Harrell, *Leukemia* **2007**, *21*, 489–493.
[19] F. Girdler, F. Sessa, S. Patercoli, F. Villa, A. Musacchio, *Chem. Biol.* **2008**, *15*, 552–562.
[20] S. Ding, N. S. Gray, X. Wu, Q. Ding, P. G. Schultz, *J. Am. Chem. Soc.* **2002**, *124*, 1594–1596.
[21] G. M. Cheetham, R. M. Knegtel, J. T. Coll, S. B. Renwick, L. Swenson, *J. Biol. Chem.* **2002**, *277*, 42419–42422.
[22] C. Ditchfield, V. L. Johnson, A. Tighe, R. Ellston, C. Haworth, *J. Cell Biol.* **2003**, *161*, 267–280.
[23] F. Girdler, K. E. Gascoigne, P. A. Eyers, S. Hartmuth, C. Crafter, *J. Cell Sci.* **2006**, *119*, 3664–3675.
[24] E. A. Harrington, D. Bebbington, J. Moore, R. K. Rasmussen, A. O. Ajose-Adeogun, *Nat. Med.* **2004**, *10*, 262–267.
[25] S. Hauf, R. W. Cole, S. LaTerra, C. Zimmer, G. Schnapp, *J. Cell Biol.* **2003**, *161*, 281–294.
[26] S. Mhaske, N. Argade, *J. Org. Chem.* **2004**, *69*, 4563–4566.
[27] Q. Chao, L. Deng, H. Shih, L. Leoni, D. Genini, *J. Med. Chem.* **1999**, *42*, 3860–3873.
[28] M. Hayakawa, H. Kaizawa, H. Moritomo, T. Koizumi, T. Ohishi, *Bioorg. Med. Chem.* **2006**, *14*, 6847–6858.
[29] A. Bridges, H. Zhou, D. Cody, G. Rewcastle, A. McMichael, *J. Med. Chem.* **1996**, *39*, 267–276.
[30] M. Tobe, Y. Isobe, H. Tomizawa, T. Nagasaki, H. Takahashi, *Bioorg. Med. Chem.* **2003**, *11*, 383–391.
[31] A. Tsvetkov, G. Latyshev, N. Lukashev, I. Beletskaya, *Tetrahedron Lett.* **2002**, *43*, 7267–7270.
[32] S. Giorgi-Renault, J. Renault, P. Gebel-Servolles, M. Baron, C. Paoletti, *J. Med. Chem.* **1991**, *34*, 38–46.
[33] I. Beletskaya, A. Cheprakov, *Chem. Rev.* **2000**, *100*, 3009–3066.
[34] R. Chinchilla, C. Nájera, *Chem. Rev.* **2007**, *107*, 874–922.
[35] L. Orfi, F. Waczek, J. Pato, I. Varga, B. Hegymegi-Barakonyi, R. Houghten, G. Keri, *Curr. Med. Chem.* **2004**, *11*, 2549–2553.
[36] V. Colandrea, S. Edmondson, R. Mathvink, A. Mastracchio, A. Weber, *PCT Int. Appl.* **2004**, *WO 2004043940*.
[37] A. D. McAinsh, P. Meraldi, V. M. Draviam, A. Toso, P. K. Sorger, *EMBO J.* **2006**, *25*, 4033–4049.
[38] R. Bayliss, T. Sardon, I. Vernos, E. Conti, *Mol. Cell* **2003**, *12*, 851–862.

Received: September 5, 2008

 © 2009 Wiley-VCH Verlag GmbH & Co. KGaA, Weinheim